

THE UNIVERSITY OF CALGARY

Frequency Sequence Spread Spectrum

by

Sassan Tabatabaei Zavareh

A THESIS

**SUBMITTED TO THE FACULTY OF GRADUATE STUDIES
IN PARTIAL FULFILLMENT OF THE REQUIREMENTS FOR THE
DEGREE OF MASTER OF SCIENCE**

**DEPARTMENT OF ELECTRICAL AND COMPUTER
ENGINEERING**

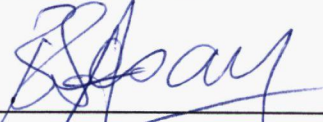
CALGARY, ALBERTA

SEPTEMBER, 1994

© Sassan Tabatabaei Zavareh 1994

THE UNIVERSITY OF CALGARY
FACULTY OF GRADUATE STUDIES

The undersigned certify that they have read, and recommend to the Faculty of Graduate Studies for acceptance, a thesis entitled, "Frequency Sequence Spread Spectrum," submitted by Sassan Tabatabaei Zavareh in partial fulfillment of the requirements for the degree of Master of Science.



Dr. Abu. Sesay, Supervisor
Department of Electrical & Computer Engineering



Dr. Michel Fattouche
Department of Electrical & Computer Engineering



Dr. R. S. Ambagaspitva
Department of Mathematics and Statistics

October 4, 1994

Abstract

In this thesis a new method of spread spectrum is described which is based on repetition of a narrowband signal in subsequent subcarriers, forming a wideband signal. A unique sequence of phase is assigned to each user to distinguish them. This technique is called frequency sequence spread spectrum (FS-SS). Two versions of FS-SS are introduced: non-overlapping FS-SS, where there is no overlap between adjacent channels and overlapping FS-SS in which certain amount of overlap is allowed. First and second moments of co-user interferences are analysed in both situations, when they are used in a CDMA system, assuming Gaussian channel. Some sets of phase sequences which provide low co-user interference peaks are also investigated.

Acknowledgements

I would like to thank my supervisor Dr A. Sesay for the support and advice he offered me generously. I also thank all of professors of the department whom I enjoyed their guidance during my studies. Thanks also to all of my friends whose comments helped me to broaden my view in my work. I would also like to thank The Ministry of Culture and Higher Education of Islamic Republic of Iran for the opportunity and financial support they provided for me to do my studies.

Dedication

To My Wonderful Parents

Table of Contents

Approval Page	ii
Abstract	iii
Acknowledgements	iv
Dedication	v
Table of Contents	vi
List of Tables	viii
List of Figures	ix
1 Introduction	1
1.1 Spread Spectrum	1
1.2 History	3
1.3 Cellular Mobile Communications	4
1.4 Objectives of the Thesis	4
1.5 Spread Spectrum Techniques	5
1.5.1 Frequency Hopping Spread Spectrum	5
1.5.2 Direct Sequence Spread Spectrum	6
1.5.3 Time Hopping	7
1.5.4 Frequency Sequence Spread Spectrum	7
1.6 Scope of the Thesis	8
2 Frequency Sequence Spread Spectrum	10
2.1 Introduction	10
2.2 Spreading Mechanism	11
2.3 Co-User Interferences	18
2.4 Overlapping Subbands	18
2.5 FS-SS and OFS-SS Performance Using Square Root Raised Cosine (SRRC) Signaling	22
2.5.1 Non-overlapping FS-SS	24
2.5.2 Overlap FS-SS	27

3	Code Design	34
3.1	Introduction	34
3.2	Definitions and Observations	35
3.3	Pseudorandom Sequences	37
3.3.1	Groups	39
3.3.2	Rings	43
3.3.3	Fields	44
3.3.4	Maximal Length Sequences	44
3.4	Code Performances	46
3.4.1	Non-overlap FS-SS Codes	47
3.4.2	Overlap FS-SS Codes	48
3.5	Conclusion	58
4	Conclusions	66
4.1	Spreading Mechanism Comparison	67
4.2	Co-user Interferences	68
4.3	Phase Sequences	68
4.4	Suggestions For Future Work	69
	Bibliography	70
A	Cosine Auto-correlation	73
A.1	Cosine Auto-correlation Formula	73
A.2	Cosine Auto-correlation Peaks	73
B	FS-SS	77
B.1	Effect of Incremental Patterns in Code Sequences on Cosine Cross-correlation Function	77
B.2	Proof of Lemma 3.1	78
C	Co-user Interference In FS-SS And OFS-SS Using Square Root Raised Cosine Signaling	79
C.1	Co-user Interference in Non-Overlapping FS-SS	80
C.2	Co-user Interference in Overlapping FS-SS	82

List of Tables

2.1	OFS-SS co-user interference components for $\alpha = 0.35$	29
2.2	OFS-SS co-user interference components for $\alpha = 0.5$	29
2.3	OFS-SS co-user interference components for $\alpha = 0.65$	29
2.4	OFS-SS co-user interference components for $\alpha = 1$	30
2.5	DS-SS and FS-SS capacity comparison	33
3.1	Maxima and minima of peak cosine auto- and cross-correlations for m-sequences for $p = 2$	49
3.2	<i>(Table 3.1, Cont'd)</i> , Maxima and minima of peak cosine auto- and cross-correlations for m-sequences for $p = 2$	50
3.3	Maxima and minima of peak cosine auto- and cross-correlations for m-sequences for $p = 3$	51
3.4	<i>(Table 3.3, Cont'd)</i> Maxima and minima of peak cosine auto- and cross-correlations for m-sequences for $p = 3$	52
3.5	Maxima and minima of peak cosine auto- and cross-correlations for m-sequences for $p = 5$	53
3.6	Maxima and minima of peak cosine auto- and cross-correlations for m-sequences for $p = 7$	54
3.7	<i>(Table 3.6, Cont'd)</i> Maxima and minima of peak cosine auto- and cross-correlations for m-sequences for $p = 7$	55
3.8	Cross-correlation peaks of Gold codes in DS-SS	59

List of Figures

2.1	Transmitter diagram for FS-SS.	12
2.2	Spreading mechanism in FS-SS ($\omega_d = 2W$).	13
2.3	An example of $Env[g_k(t)]$ for $N = 63$	14
2.4	Cosine auto-correlation factor versus $\phi_d^l = \omega_d \tau_l$ for $N = 31$	17
2.5	Spectra for overlapping signals.	21
2.6	Bandwidth of OFS-SS signals	22
2.7	Diagram of a FS-SS system	23
2.8	Square root raised cosine pulse shape in time and frequency domain.	25
2.9	Capacity of a FS-SS CDMA using SRRC signaling versus overlapping coefficient η for different values of α	32
3.1	Effect of incremental patterns in phase sequences on cosine cross-correlation: a) $N = 127, N_1 = 10, N_2 = 52, \psi = \pi, L = 2$ b) $N = 56, N_1 = 8, N_2 = 49, \psi = 0, L = 3$	38
3.2	Vector representation of cosine cross-correlation behavior.	39
3.3	$R(\phi, s)$ versus $\phi = \omega_d \tau$ for a typical m-sequence s , generated by $f(x)$ in equation (3.5) and initial value 10000.	60
3.4	$\max(R(\phi, T^i s))$ for set $S[f]$ generated by $f(x)$ in equation (3.5)	61
3.5	Cosine cross-correlation peaks for coset generated by $f = 101111$, and $g = 111101, v_{i_0} = 10000$. $N = 31$	62
3.6	Cosine cross-correlation peaks for coset generated by $f = 1100001$, and $g = 1110011, v_{i_0} = 100000$. $N = 63$	63
3.7	Cosine cross-correlation peaks for coset generated by $f = 11000001$, and $g = 10111111, v_{i_0} = 1000000$. $N = 127$	64
3.8	Cosine cross-correlation peaks for coset generated by $f = 101110001$, and $g = 101011111, v_{i_0} = 10000000$. $N = 255$	65
A.1	Vector representation of cosine auto-correlation.	74
A.2	Cosine auto-correlation function for $N = 8$	75

Chapter 1

Introduction

1.1 Spread Spectrum

Spread Spectrum (SS) is a modulation-demodulation technique [1] with some unique characteristics which make it attractive for applications such as: military communications, guidance systems, ranging, multiple access systems etc. A definition of spread spectrum that adequately reflects these characteristics, is as follows [2]:

Spread spectrum is a means of transmission in which the signal occupies a bandwidth much larger than the minimum necessary to send the information. The band spread is accomplished by means of a code which is independent of the data, and a synchronized reception with the code at receiver is used for despreading and subsequent data recovery.

Spread spectrum is typically designed to be transparent to other users, i.e., spread spectrum signals are designed to provide negligible interference to the communication of other existing users and indeed, it is difficult to determine if a spread spectrum signal is actually present [3].

Note that for any spread spectrum system to operate properly, it is necessary for the receiver to acquire the correct phase position of the incoming waveform, and it must continually track that phase position so that loss of lock will not occur. The two processes of acquisition and tracking form the synchronization subsystem of a spread spectrum receiver.

There are many reasons for spreading the spectrum; some of the benefits it provides, are:

- Antijamming
- Anti-interference
- Low probability of intercept
- Multiple access capability
- High resolution ranging

Although in recent years civilian applications of spread spectrum such as code division multiplexing for cellular mobile communications, is being investigated by research and industrial communities, historically it has its roots in military communications. In the next section a brief history of spread spectrum technique is reviewed.

1.2 History

The first notions of spread spectrum go back to times as early as 1920[4], as U.S patent office records suggest, but the techniques found by that time did not have all the characteristics of spread spectrum. Between the two world wars, a number of independent researchers in different countries indicated that modulating a signal with a pseudo-noise signal can provide immunity against some unwanted interferences. Noise, in the sense that these signals behave like noise, and pseudo because these signals could be reconstructed by deterministic means in the receiver.

During world war II, where disruption of communications by enemy's jamming was frustrating, and interception of important messages could endanger some operations, a great amount of research was initiated to find an antijamming secure communications technique [5]. Although engineers in the military developed some methods such as changing carrier frequency periodically (similar to frequency hopping SS), it was around mid 1950's that spread spectrum entered into the technical terminology as it is known conventionally [2]. A more comprehensive review of the interesting history of spread spectrum can be found in [4].

Until 1980, SS was almost totally restricted to military applications. In 1983, in the U.S a special band was allocated for commercial SS [3], and that encouraged researchers to start experimenting on civilian applications of SS. Some results were suggesting that SS can be a solution for the problem of spectral congestion, which is a limiting factor in further expansion of wireless communications, in some cases. One example of such cases is cellular mobile communications. Spread spectrum is also able to combat some severe conditions of mobile radio channels, such as multipath

[6] and fading.

1.3 Cellular Mobile Communications

In a cellular system, the area of coverage is divided into a number of smaller regions (cells); each one covered by a base-station. Any mobile in a cell communicates with its respective base station to access the telephone network. When frequency division multiple access (FDMA) or Time division multiple access (TDMA) are used for multiplexing different users, to reduce interference, a frequency band used in a cell cannot be re-used in the first neighboring cells. This limits the capacity of the whole system. Theoretically, spread spectrum code division multiple access (SS-CDMA) allows a number of users to use the same frequency band, and therefore a higher frequency re-use factor (and consequently system capacity) is expected [7] [8] [9]. However, it is almost impossible to design completely orthogonal spread spectrum waveforms, for all possible relative delays, for all the users; therefore any receiver will experience some interference from co-users. These interferences combined with near-far effect [10], limit the capacity of CDMA system severely.

1.4 Objectives of the Thesis

To combat the problem mentioned in last section, multi-user detection [11] has been proposed, in which the receiver tries to reduce co-user interferences by using its knowledge of co-users spreading waveforms and system specifications. The disadvantage of this scheme is considerable complexity. Another approach is to use SS techniques that produce less co-user interferences. Although researchers have found

some good sequences and waveforms for existing SS techniques, for further improvement of SS-CDMA systems, it seems necessary to search for new techniques with potential for better performance. This thesis investigates a new SS technique, namely frequency sequence spread spectrum, in terms of its co-user interference performance.

1.5 Spread Spectrum Techniques

The most commonly used SS techniques are Frequency hopping SS (FH-SS), direct sequence SS (DS-SS), and less used method of time hopping SS (TH-SS) [1] [12] [2]. Much research has been done on these techniques, especially on DS-SS, for CDMA purposes [13]. Although some good set of codes have been found for these techniques [14], any further reduction of co-user interferences can help to improve the capacity of a CDMA system.

In this thesis, a new technique of SS referred to as 'Frequency sequence spread spectrum' is introduced and some of its properties are investigated. Before going into details, it seems necessary to have a background on existing spread spectrum methods.

1.5.1 Frequency Hopping Spread Spectrum

FH spread spectrum utilizes the large spectrum provided for spread spectrum systems by periodically changing the carrier frequency of the transmitted signal. The changing is called 'hopping'. If the entire allocated bandwidth is, say, 1000 times wider than the bandwidth of the transmitted signal, then during a given time interval the signal can be transmitted at any one of 1000 possible frequencies. The result

is reduced interference to any existing user. For example, if an existing narrowband user occupies one of the 1000 frequency slots, then interference with the existing user occurs only 1/1000 of the total time. During the remaining time, the transmission has hopped to different frequencies and, therefore, does not cause interference.

There are two basic hopping patterns; one called fast hopping which makes two or more hops for each symbol. The other called slow hopping which transmits two or more symbols for each hop. FH with slow hopping does not serve the purpose of increasing capacity in cellular CDMA system [10]. The slow hopping is to let good channels downgrade and bad channels upgrade. If bad channels do occur in this high capacity SS system, the system does not provide normal channels with excessive signal levels which can average with the poor signal levels of those bad channels to within an acceptable quality level. The fast hopping does help increase the capacity because of its advantage of applying diversity, but the technology to have fast hopping at high frequencies is not available.

1.5.2 Direct Sequence Spread Spectrum

Direct-sequence spread spectrum achieves a spreading of the spectrum by modulating the original signal with a very wideband signal relative to the data bandwidth. This wideband signal can be chosen to have two possible amplitudes $+1$ and -1 , and these amplitudes are switched, in a pseudorandom manner, periodically. Thus at each equally spaced interval, a decision is made as to whether the wideband modulating signal should be $+1$ or -1 . If a coin were tossed to make such a decision, the resulting sequence would be truly random. However, in such a case, the receiver would not know the sequence a priori and could not properly receive the transmis-

sion. Instead, an approximately random sequence, called pseudorandom sequence is generated electronically. This PN sequence is known a priori to the transmitter and receiver.

For a set of codes in DS-SS to perform well, not only auto- and cross-correlation, but also the partial cross-correlations of any two codes should be small [15]. Large peaks of partial cross-correlation can lengthen synchronization time, and if they happen frequently, large co-user interferences will occur. A considerable amount of research has been done on sequences for DS-SS [14] which has led to sets of sequences with reasonably good auto- and cross-correlation properties such as Gold codes, small sets of Kasami codes and some Gold-like codes. Some complex multilevel sequences also have been proposed with good properties [16]. However, still better codes are needed for more improvement in CDMA system capacity.

1.5.3 Time Hopping

A message transmitted with a data rate of R requiring a transmit time interval T is now allocated a longer transmission time interval T_s . In time T_s , the data are sent in bursts dictated by a hopping pattern. The time interval between bursts t_n also can be varied. The time spreading data rate R_s is always less than the information bit rate R . TH-SS is not used for CDMA applications due to difficulties in synchronization.

1.5.4 Frequency Sequence Spread Spectrum

Frequency sequence spread spectrum (FS-SS) is a new spread spectrum technique which this thesis is focused on. FS-SS spreads the signal spectrum by repeating the narrowband signal in frequency domain at equidistant bands. The phase of the signal

in each band is offset by a certain value. Each user has a unique sequence of phases in subsequent subbands. At the desired receiver, this signal is demodulated using a synchronized replica of the spreading waveform, and therefore all the subbands add up in baseband while aligned, performing despreading function. For any co-user, the subbands translated to baseband are not aligned, and consequently a smaller signal is produced. The cosine cross correlation of any two phase sequences, defined in next chapter, determines the peaks of interference from a co-user.

Two distinct cases of FS-SS are investigated. Non-overlapping FS-SS in which there is no overlap between neighboring subbands, and overlapping FS-SS (OFS-SS) where certain amount of overlap is allowed. OFS-SS occupies less bandwidth than FS-SS for the same number of subbands, but it introduces more co-user interference.

1.6 Scope of the Thesis

In this thesis, FS-SS is introduced and investigated as a new spread spectrum technique. The main emphasis is on the performance of this technique in terms of peaks and power of co-user interference. In Chapter 2, the principles of spreading and despreading in FS-SS are explained. Also, as an example of co-user interference, a two user CDMA system using square root raised cosine signaling is investigated. It is shown that for non-overlapping FS-SS, the co-user interference power is independent of users' phase sequences.

Chapter 3 examines different phase sequences and their properties in FS-SS and also in OFS-SS. Maximal length sequences, used in other spread spectrum methods are also used in this case ; therefore a quick review of groups, cosets and finite fields

is presented too. Peaks of performance functions, referred to as cosine auto- and cross-correlation, of sequences in FS-SS are listed in this chapter.

In Chapter 4, as a conclusion, a comparison has been made between FS-SS properties and those of other spread spectrum techniques.

Chapter 2

Frequency Sequence Spread Spectrum

2.1 Introduction

Different spread spectrum techniques have been developed for different applications. While Frequency-Hopping is more popular in military communications, Direct-Sequence seems to have attracted more attention for civilian applications such as CDMA. Time-Hopping spread spectrum is not widely used due to synchronization problems.

FS-SS is a new spread spectrum technique in which spreading is controlled in the frequency domain rather than in the time domain. In FS-SS the information signal is modulated by a set of subcarriers, but unlike FH-SS it is transmitted simultaneously in time, and unlike DS-SS with periodic code, spreading is achieved by a sequence of subbands.

In this chapter, the principles of FS-SS, spreading and despreading mechanisms

and some of their properties are explained.

2.2 Spreading Mechanism

As in any other spread spectrum technique, FS-SS also results from modulation of information signal by a wideband spreading signal. This wideband code, in FS-SS, is chosen to be a series of impulses in the frequency domain located at equidistant frequencies. The uniform frequency spacing guarantees periodicity of the spreading signal which is essential in fast synchronization. A random sequence of phases is also attributed to the impulse sequence which is, in fact, the unique characteristic of the signal. This is important in CDMA systems in order to distinguish between different users and reject undesired ones. Although the amplitudes of impulses can also be variable, in this thesis they are considered the same for all subcarriers. The reason is to produce an almost flat signal power spectrum.

Let us assume our data signal is narrowband with a baseband bandwidth of W . Modulating it with a sequence of equidistant subcarriers creates a sequence of subbands carrying the same information and together form a wideband signal. The basic transmitter for a FS-SS signal is shown in Figure 2.1. For user k , the information signal is

$$d_k(t) = \sum_{i=-\infty}^{+\infty} d_i^k p(t - iT), \quad d_i^k = \pm 1 \quad (2.1)$$

where $p(t)$ is the pulse shape, and d_i^k is the i th data symbol. The spreading signal is:

$$q_k(t) = \sum_{i=0}^{N-1} \cos[(\omega_{IF} + i\omega_d)t + \theta_i^k], \quad \theta_i^k \in F[L] \quad (2.2)$$

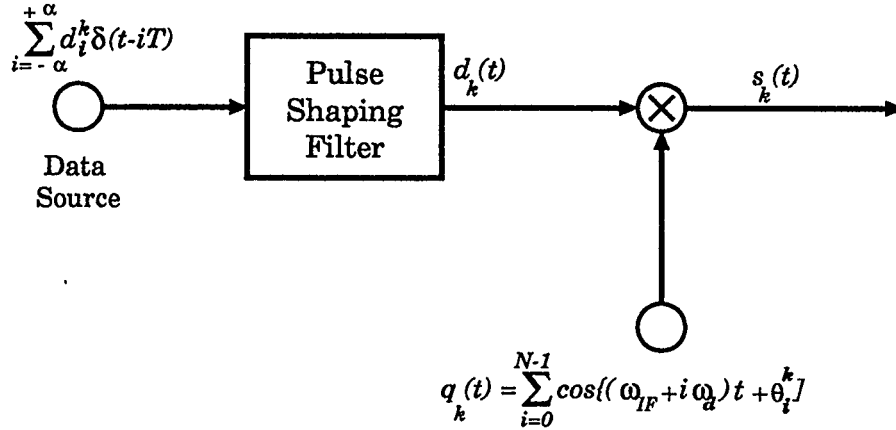


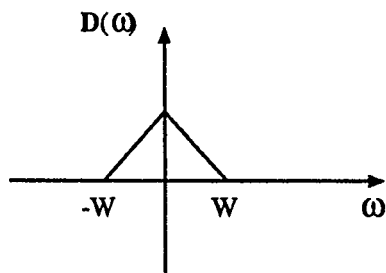
Figure 2.1: Transmitter diagram for FS-SS.

where $F[L] = \{0, \frac{2\pi}{L}, \frac{2(2\pi)}{L}, \dots, \frac{(L-1)(2\pi)}{L}\}$, and the resulting spread spectrum signal is:

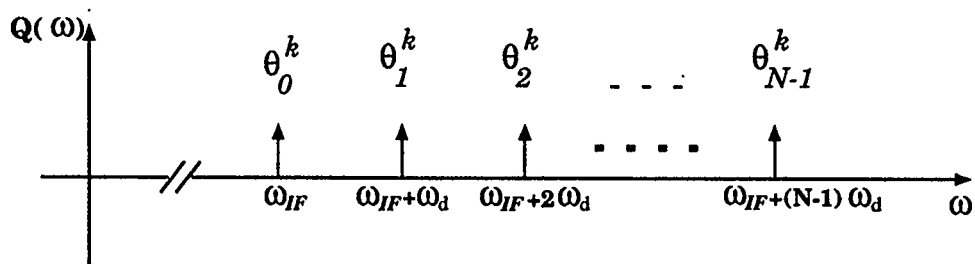
$$s_k(t) = d_k(t)q_k(t)$$

The phase sequence $\Theta^k = \theta_0^k \theta_1^k \dots \theta_{N-1}^k$, is the k th user code and should be chosen in such a way to produce as little interference as possible on the other users' receivers. Figure 2.2 shows how the signal is spread assuming $\omega_d = 2W$, i.e. there is no overlap between adjacent subbands. The spreading process should be carried out at an IF band, otherwise the RF required bandwidth for FS-SS signal will be twice as much as the case when spreading is done at baseband.

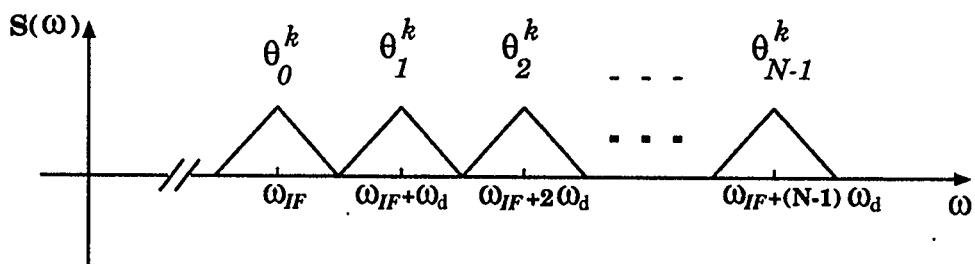
The FS-SS signal is modulated to RF band and transmitted. Since most RF amplifiers are non-linear or have a limited range of linearity, large instantaneous peaks in the modulating signal ($q_k(t)$) should be avoided. The envelope of $q_k(t)$ is



a) Baseband information signal spectra



(b) Spectrum of spreading Signal



c) Wideband Spectra

Figure 2.2: Spreading mechanism in FS-SS ($\omega_d = 2W$).

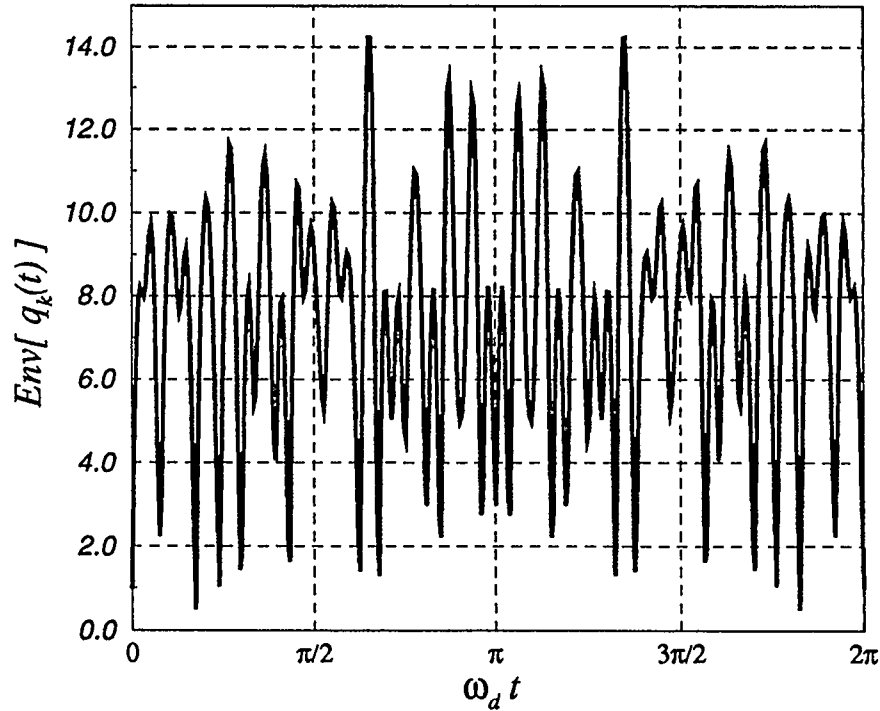


Figure 2.3: An example of $Env[q_k(t)]$ for $N = 63$.

obtained as:

$$\begin{aligned}
 q_k(t) &= \text{Re}\{\sum_{i=0}^{N-1} \exp[j(\omega_{IF}t + i\omega_d t + \theta_i^k)]\} \\
 &< |\sum_{i=0}^{N-1} \exp[j(i\omega_d t + \theta_i^k)]| \\
 &= Env[q_k(t)]
 \end{aligned}$$

Figure 2.3 shows an example of $Env[q_k(t)]$ for $N = 63$ and $\Theta^k = \pi(m^k)$ where m^k is a binary m-sequence. The example shows that $Env[q_k(t)]$ is nonconstant, however, with a proper choice of phase sequence $\Theta^k = \theta_0^k, \dots, \theta_{N-1}^k$, large peaks of this envelope can be prevented. In other words the exponential components will not be aligned at any time.

In the receiver, after demodulation to the IF band, despreading is accomplished by multiplication of the received signal with a replica of $q_k(t)$. Assuming only the k th user is transmitting, the despread signal for a Gaussian channel is:

$$\begin{aligned}
r_k(t) &= s_k(t - \tau_k)q_k(t) \\
&= d_k(t - \tau_k)q_k(t - \tau_k)q_k(t) \\
&= d_k(t - \tau_k)(\sum_{j=0}^{N-1} \cos[(\omega_{IF} + j\omega_d)(t - \tau_k) + \theta_j^k])(\sum_{i=0}^{N-1} \cos[(\omega_{IF} + i\omega_d)t + \theta_i^k]) \\
&= d_k(t - \tau_k)\{\sum_{j=0}^{N-1} \sum_{i=0}^{N-1} \frac{1}{2}[\cos[(i - j)\omega_d t + (\theta_i^k - \theta_j^k) + \omega_{IF}\tau_k + j\omega_d\tau_k] \\
&\quad + \cos[(2\omega_{IF} + (i + j)\omega_d)t + (\theta_i^k + \theta_j^k) - \omega_{IF}\tau_k - j\omega_d\tau_k]]\}
\end{aligned} \tag{2.3}$$

where τ_k is the signal delay due to asynchronous transmission. If the despreading signal is synchronized with the received signal, we can set $\tau_k = 0$. Passing the product through a low pass filter with $f_{cutoff} = W$, all the components at $2\omega_{IF}$ and $\{n\omega_d, n \neq 0\}$ are attenuated and the result is $y_k(t)$:

$$\begin{aligned}
y_k(t) &= r_k(t) * h(t) \\
&= \frac{1}{2} \hat{d}_k(t) \sum_{i=0}^{N-1} \cos(\theta_i^k - \theta_i^k) \\
&= \frac{N}{2} \hat{d}_k(t)
\end{aligned} \tag{2.4}$$

where

$$\hat{d}_k(t) = d_k(t) * h(t)$$

and $h(t)$ can be an ideal low pass filter or a matched filter matched to the pulse shape $p(t)$. In the case of imperfect synchronization $\tau_k \neq 0$, then the despread signal is:

$$y_k(t) = \frac{1}{2} \hat{d}_k(t - \tau_k) \sum_{i=0}^{N-1} \cos(\phi_{IF}^k + i\phi_d^k) \tag{2.5}$$

where $\phi_d^k = \omega_d\tau_k$ and $\phi_{IF}^k = \omega_{IF}\tau_k$ are random phases. Since the summation term in equation (2.5) play a role similar to auto-correlation function in DS-SS, let us call

it cosine auto-correlation factor and denote its absolute value by $AM(\phi_d^k)$. AM can be bounded by the function AMX :

$$\begin{aligned}
AM(\phi_d^k) &= \left| \sum_{i=0}^{N-1} \cos(\phi_{IF}^k + i\phi_d^k) \right| \\
&= \left| \text{Re} \left\{ \sum_{i=0}^{N-1} \exp[j(\phi_{IF}^k + i\phi_d^k)] \right\} \right| \\
&< \left| \exp[j(\phi_{IF}^k)] \cdot \sum_{i=0}^{N-1} \exp[j(i\phi_d^k)] \right| \quad (2.6) \\
&= \left| \sum_{i=0}^{N-1} \exp[j(i\phi_d^k)] \right| \\
&= AMX(\phi_d^k)
\end{aligned}$$

and it can be shown (Appendix A) that:

$$\begin{aligned}
AMX(x) &= \left| \sum_{i=0}^{N-1} \exp[j(ix)] \right| = \left| \frac{\sin(Nx/2) \cos[(N-1)x/2]}{\sin(x/2)} - j \frac{\sin(Nx/2) \sin[(N-1)x/2]}{\sin(x/2)} \right| \\
&= \left| \frac{\sin(Nx/2)}{\sin(x/2)} \right| \quad (2.7)
\end{aligned}$$

Figure 2.4 shows the variations of $AMX(\phi_d^k)$ versus ϕ_d^k for $N = 31$. After some analysis, the ratio of the m -th peak (AP_m) to the main peak for sufficiently large N ($N > 10$) is found to be (Appendix A) approximately:

$$AR_m = \frac{|AP_m|}{|AP_0|} = \frac{2}{\pi(2m+1)}, \quad m \neq 0, \quad m < N/6$$

and the worst case AR_{max} is :

$$AR_{max} = MAX(AR_m) = \frac{2}{3\pi} = 0.212$$

The parameter AM is equivalent to the auto-correlation of sequences in DS-SS, therefore, it is possible to compare AR_{max} with the ratio of the largest auto-correlation peak for $\tau > T_c$ (chip time) to the same value for $\tau = 0$ in DS-SS ($Auto_{max}$). Assuming Gold codes being used in DS-SS, AR_{max} is smaller than $Auto_{max}$ for the spreading ratios (SR) less than 63. As SR increases $Auto_{max}$ decreases whereas

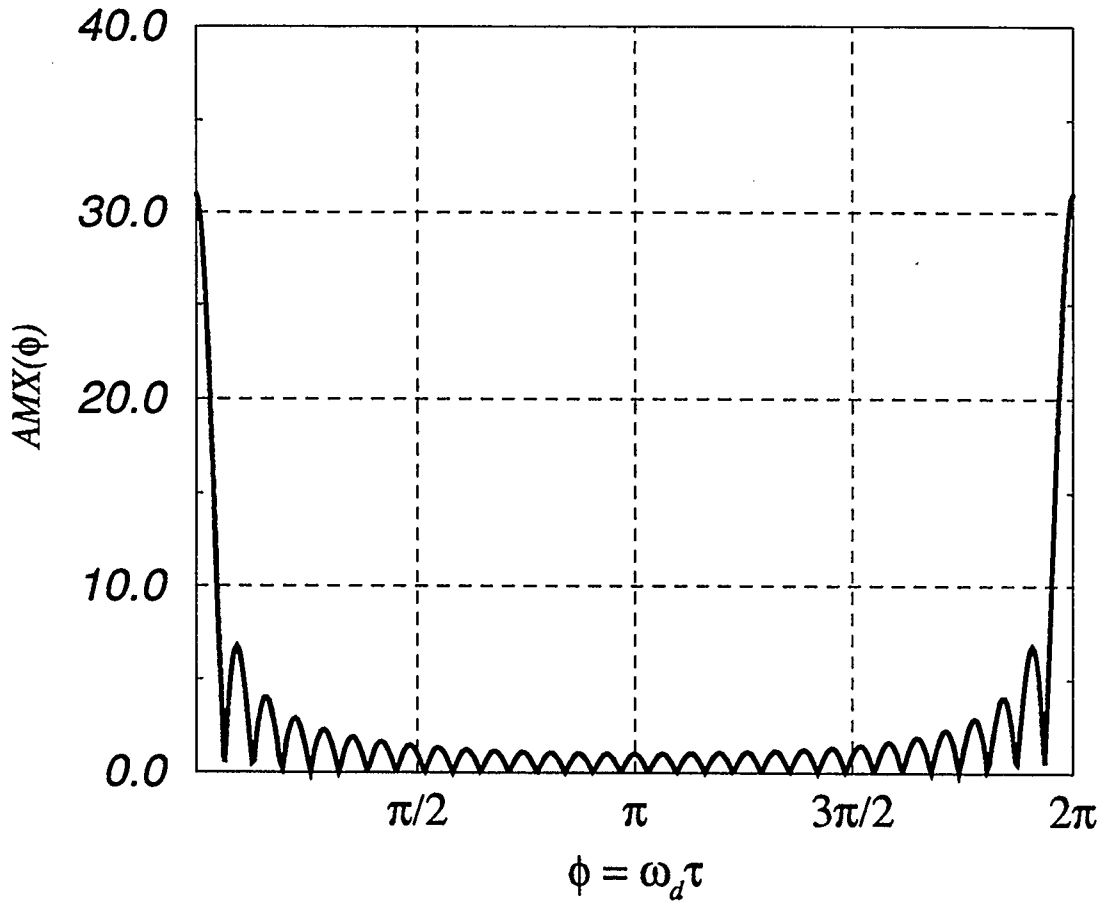


Figure 2.4: Cosine auto-correlation factor versus $\phi_d^l = \omega_d \tau_l$ for $N = 31$

AR_{max} remains the same. This fact suggests that FS-SS can offer better performance for small spreading ratios in rejecting multipath signals. In Section 3.4.2, AP_2 is listed for different values of N .

2.3 Co-User Interferences

In CDMA systems, co-users cause some interferences in each other's receiver. On a Gaussian channel, the interference contributed by the l th user at the k th receiver can be represented as:

$$\begin{aligned} I_l(t) &= [s_l(t - \tau_l)q_k(t)] * h(t) \\ &= \frac{1}{2}\hat{d}_l(t - \tau_l) \sum_{i=0}^{N-1} \cos[\phi_{IF}^l + i\phi_d^l + (\theta_i^k - \theta_i^l)] \end{aligned}$$

The amount of this interference is directly proportional to the factor:

$$AI(\phi_d^l) = \sum_{i=0}^{N-1} \cos(\phi_{IF}^l + i\phi_d^l + \theta_i^{kl})$$

where $\phi_d^l = \omega_d \tau_l$, $\phi_{IF}^l = \omega_{IF} \tau_l$, and $\theta_i^{kl} = \theta_i^k - \theta_i^l$ is another sequence of phases in the set $F[L]$. Using the same approach as in equation (2.6) gives the bound:

$$AI(\phi_d^l) < \left| \sum_{i=0}^{N-1} \exp[j(i\phi_d^l + \theta_i^{kl})] \right| = AIX(\phi_d^l) \quad (2.8)$$

where AIX can be called cosine cross-correlation factor (Chapter 3). The cosine cross-correlation factor peak can be reduced by a careful choice of the sequences $\{\theta^k\}$ and $\{\theta^l\}$. If all the users are synchronized, the orthogonal codes (which results in $AIX(0) = 0$) are the best; However, in many systems, transmission is asynchronous and the best codes which produce minimum interference should be searched for.

2.4 Overlapping Subbands

In the last section it was assumed that there is no overlap between adjacent subbands. Now let us allow some overlap of nearest neighbor subbands i.e. $W < \omega_d < 2W$ (Figure 2.5a). The advantage of overlap is bandwidth savings. After demodulating

and despreading there is an additional interference from the overlap of two adjacent subband tails (Figure 2.5b). With a proper choice of codes for users, this component for desired signal is small if synchronization has been acquired (Figure 2.5c). Using equation (2.3) the signal after low pass filtering can be written as:

$$\begin{aligned}
y_l(t) = r_l(t) * h(t) = \frac{1}{2}d_l(t - \tau_l) [& \sum_{i=0}^{N-1} \cos(i\phi_d^l + \phi_{IF}^l + \theta_i^{kl}) \\
& + \sum_{i=1}^{N-1} \cos(\omega_d t + (\theta_i^k - \theta_{i-1}^l) + \phi_{IF}^l + (i-1)\phi_d^l) \\
& + \sum_{i=1}^{N-1} \cos(-\omega_d t + (\theta_{i-1}^k - \theta_i^l) + \phi_{IF}^l + i\phi_d^l)] * h(t)
\end{aligned} \tag{2.9}$$

Two distinct components in $y_l(t)$ can be recognized: a main lobe signal ($M_l(t)$), which is the same as the interference signal in non-overlapping FS-SS, and the tail interference signal ($O_l(t)$):

$$M_l(t) = \frac{1}{2}\hat{d}_l(t - \tau_l) \left[\sum_{i=0}^{N-1} \cos(i\phi_d^l + \phi_{IF}^l + \theta_i^{kl}) \right] \tag{2.10}$$

$$\begin{aligned}
O_l(t) = \frac{1}{2}d_l(t - \tau_l) [& \sum_{i=1}^{N-1} \cos(\omega_d t + (\theta_i^k - \theta_{i-1}^l) + \phi_{IF}^l + (i-1)\phi_d^l) \\
& + \sum_{i=1}^{N-1} \cos(-\omega_d t + (\theta_{i-1}^k - \theta_i^l) + \phi_{IF}^l + i\phi_d^l)] * h(t)
\end{aligned} \tag{2.11}$$

Using Euler's formula $\cos(x) = 1/2(\exp(jx) + \exp(-jx))$ in the summations of equation (2.11), and considering only positive frequency components, the following relation is obtained:

$$\begin{aligned}
O_{ps}(t) &= \frac{1}{2}d_l(t - \tau_l) \left\{ \frac{1}{2} \left[\sum_{i=1}^{N-1} \exp(\omega_d t + (\theta_i^k - \theta_{i-1}^l) + \phi_{IF}^l + (i-1)\phi_d^l) \right. \right. \\
& \quad \left. \left. + \sum_{i=1}^{N-1} \exp(\omega_d t - (\theta_{i-1}^k - \theta_i^l) - \phi_{IF}^l - i\phi_d^l) \right] \right\} * h(t) \\
&= \frac{1}{2}(d_l(t - \tau_l) \exp(j\omega_d t)) * h(t) \left[\sum_{i=1}^{N-1} \exp(j((\theta_i^k - \theta_{i-1}^l) + \phi_{IF}^l + (i-1)\phi_d^l)) \right. \\
& \quad \left. + \sum_{i=1}^{N-1} \exp(-j((\theta_{i-1}^k - \theta_i^l) - \phi_{IF}^l - i\phi_d^l)) \right] \\
&= ov_{ps}(t).TM(\phi_d^l)
\end{aligned}$$

where $ov_{ps}(t)$ is the positive sideband of the overlap signal. Considering both sidebands of the overlap signal we have:

$$ov(t) = \frac{1}{2}[d_i(t - \tau_i) \cos(\omega_d t + \psi)] * h(t) \quad (2.12)$$

where ψ is the phase of the TM factor. Factor $TM(\phi_d^l)$ is the tail amplitude weight.

One can further obtain an upper bound on TM as:

$$\begin{aligned} |TM(\phi_d^l)| &\leq |\sum_{i=1}^{N-1} \exp[j((\theta_i^k - \theta_{i-1}^k) + (i-1)\phi_d^l)]| \\ &\quad + |\sum_{i=1}^{N-1} \exp[j((\theta_{i-1}^k - \theta_i^k) + i\phi_d^l)]| \\ &= Z(\phi_d^l, (L/2\pi)\Theta^l, (L/2\pi)\Theta^k) \end{aligned} \quad (2.13)$$

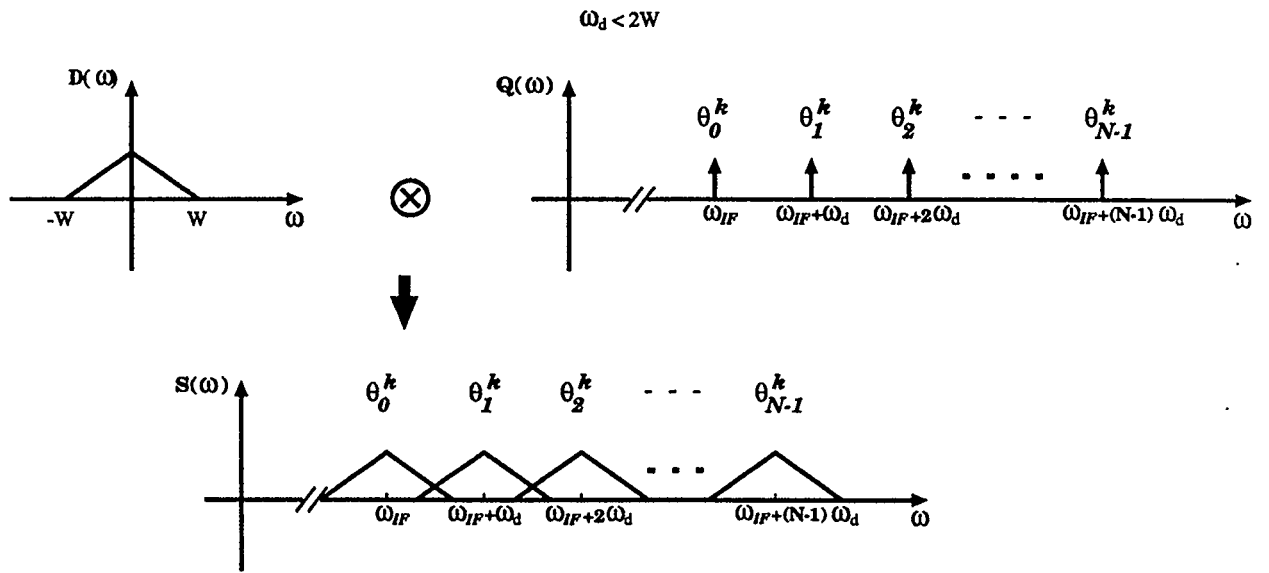
OFS-SS Bandwidth

In overlapping FS-SS (OFS-SS) signals occupy less bandwidth than in the non-overlapping case for the same number of subcarriers, but at the expense of some additional interference. From Figure 2.6, the total bandwidth of a OFS-SS signal is found to be:

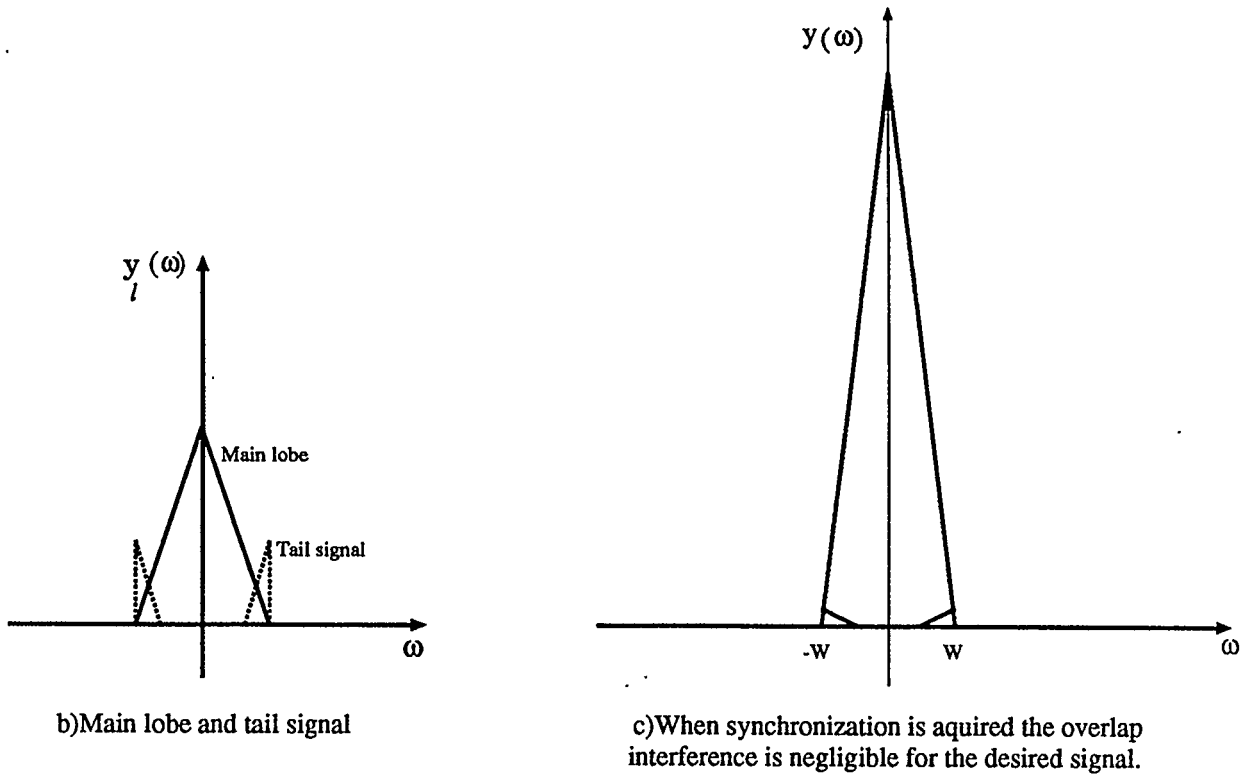
$$\begin{aligned} W_{OFS-SS} &= N\omega_d + 2W \\ &= 2W[N(1 - \eta) + \eta] \end{aligned} \quad (2.14)$$

where $\eta = 1 - \omega_d/2W$ is the overlap coefficient. $\eta = 0$ means there is no overlap whereas total overlap happens when $\eta = 1$, for which no spreading is achieved.

The average interference power due to overlapping is a function of a number of factors: the signal shape in the frequency domain, receiver filter frequency response, and η . How tolerable is this interference depends on the system using OFS-SS and the specifications set for that. In the next section a special case is investigated, where data is shaped with square root raised-cosine signal at the transmitter, and matched filter detection is used at the receiver.



a) Adjacent subbands overlap



b) Main lobe and tail signal

c) When synchronization is acquired the overlap interference is negligible for the desired signal.

Figure 2.5: Spectra for overlapping signals.

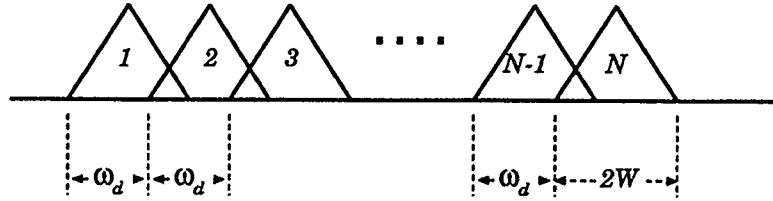


Figure 2.6: Bandwidth of OFS-SS signals .

2.5 FS-SS and OFS-SS Performance Using Square Root Raised Cosine (SRRC) Signaling

In this section the performance and behavior of FS-SS and OFS-SS system is investigated in terms of co-user interference, using SRRC signaling [17] and matched filter detection. Figure 2.7 depicts a block diagram of the system. The goal is to calculate the mean and variance of the error signal caused by co-user interference. Therefore, we assume only co-user l is interfering, and also it is assumed that perfect synchronization in despreading and sampling time are acquired at the receiver for the desired signal.

SRRC pulse shaping is used at the transmitters, because passing the signal through matched filter in the receiver produces raised cosine pulse shapes which would minimize intersymbol interference [18]. The channel is considered to be just a delay line with delay τ_l .

The l th co-user transmitted signal $s_l(t)$ is:

$$s_l(t) = [d_l(t) * p(t)]q_l(t)$$

where $q_l(t)$ is the spreading signal for user l (defined in equation (2.2)), $d_l(t)$ is the

Figure 2.7: Diagram of a FS-SS system .

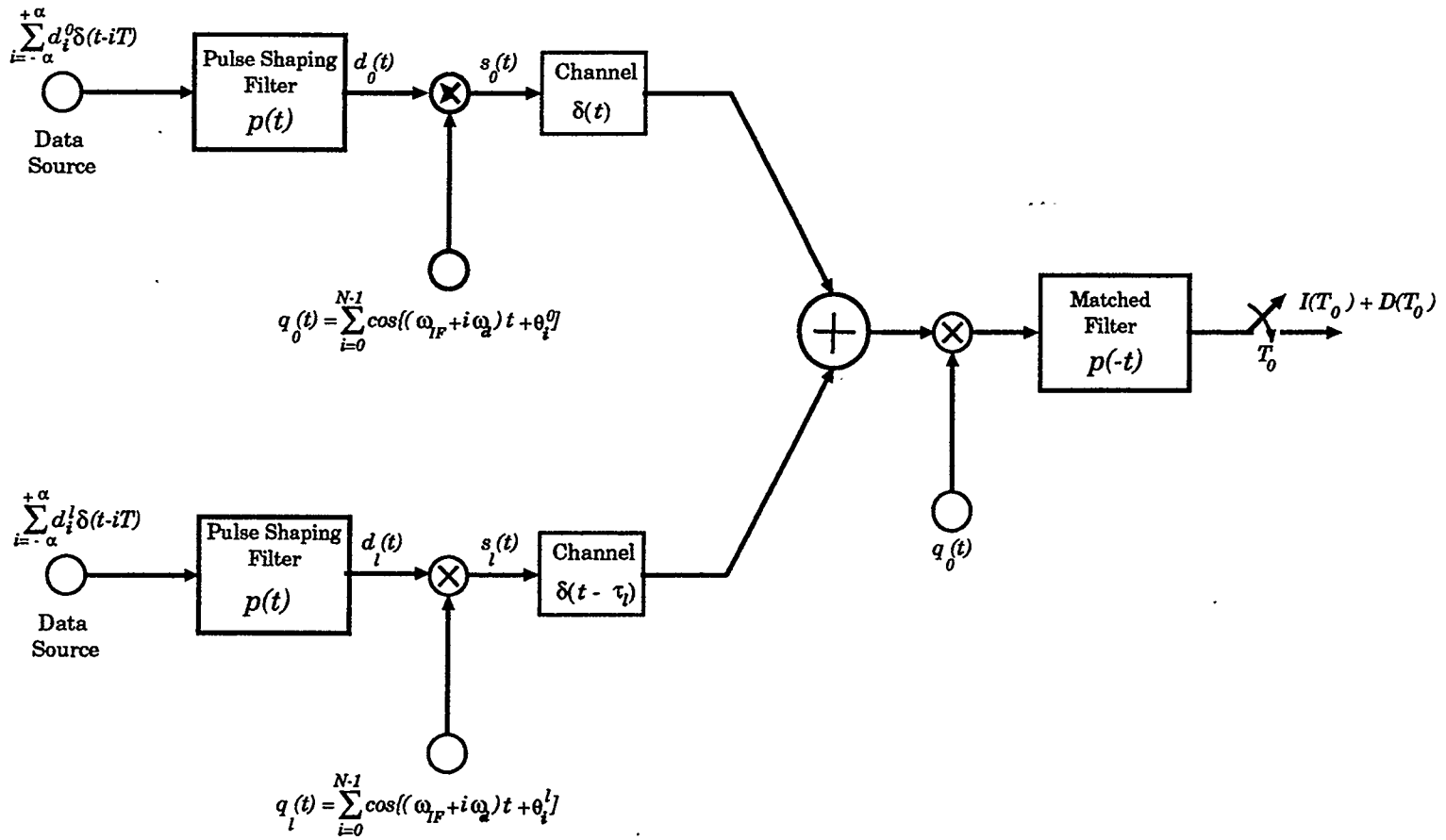


Figure 2.7: Diagram of a FS-SS system

data signal:

$$d_l(t) = \sum_{n=-\infty}^{\infty} d_n^l \delta(t - nT)$$

and $p(t)$ is SRRC filter impulse response, given by:

$$p(t) = \begin{cases} 1 - \alpha + \frac{4\alpha}{\pi}, & t = 0 \\ \frac{\alpha}{\sqrt{2}} \left[\left(1 + \frac{2}{\pi}\right) \sin\left(\frac{\pi}{4\alpha}\right) + \left(1 - \frac{2}{\pi}\right) \cos\left(\frac{\pi}{4\alpha}\right) \right], & t = \pm \frac{T}{4\alpha} \\ \frac{\sin[\pi(1-\alpha)\frac{t}{T}] + 4\alpha\frac{t}{T} \cos[\pi(1+\alpha)\frac{t}{T}]}{\pi\frac{t}{T}[1-(4\alpha\frac{t}{T})^2]}, & \text{for all other } t \end{cases}$$

while its frequency response is given by:

$$P(f) = \begin{cases} T, & 0 \leq |f| \leq \frac{1-\alpha}{2T} \\ T\sqrt{\frac{1}{2}\{1 - \sin[\frac{\pi T}{\alpha}(|f| - \frac{1}{2T})]\}}, & \frac{1-\alpha}{2T} \leq |f| \leq \frac{1+\alpha}{2T} \\ 0, & |f| > \frac{1+\alpha}{2T} \end{cases}$$

Figures 2.8 show SRRC signal in frequency and time domain, for some values of α .

2.5.1 Non-overlapping FS-SS

First, the case of non-overlapping FS-SS is investigated, where $\omega_d = 2W$.

At the receiver, the received co-user signal is modulated by the desired (the zeroth) user's despreader signal $q_0(t)$, and passes through the matched filter:

$$I_l(t) = \{[s_l(t) * h_{ch}(t)]q_0(t)\} * p(t)$$

where $I_l(t)$ is the l th co-user interference signal at the output of the matched filter, and $h_{ch}(t) = \delta(t - \tau_l)$ is the channel impulse response. Since SRRC filter is low pass, and $g(t - \tau) = (1/T)[p(t - \tau) * p(t)]$ is a raised cosine signal shape, $I_l(t)$ reduces to:

$$I_l(t) = [T \sum_{n=-\infty}^{\infty} d_l g(t - nT - \tau_l)] \left[\sum_{i=0}^{N-1} \cos(i\omega_d \tau_l + \phi_{IF} + \theta_i^{l0}) \right].$$

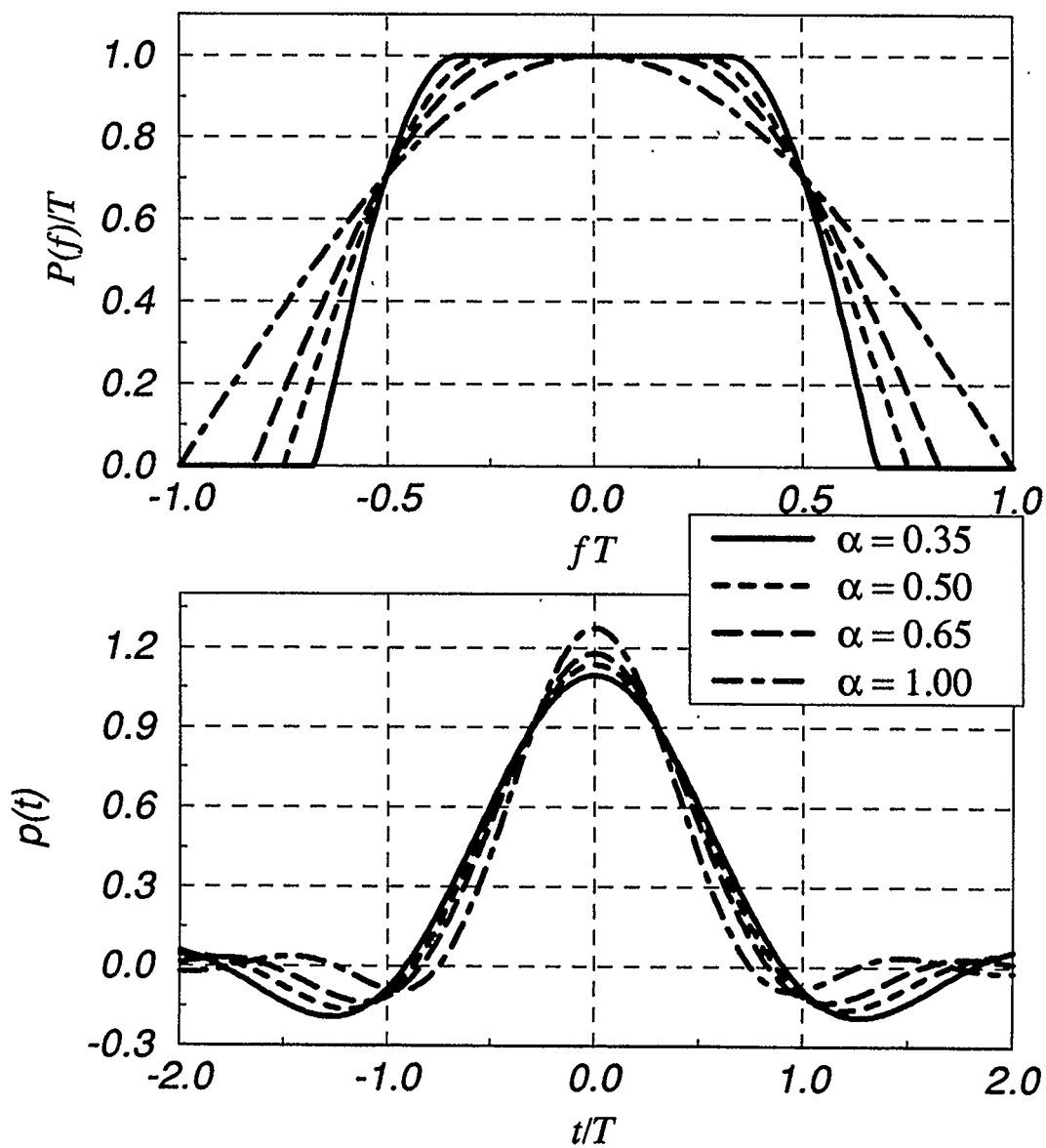


Figure 2.8: Square root raised cosine pulse shape in time and frequency domain.

Without loss of generality, let us assume the desired signal sampling time is at $t = 0$. Now, the error at the sampling time due to co-user l is I_l , which is a random variable with mean and variance $\overline{I_l}$ and $\overline{I_l^2(0)}$. At time $t = 0$, $I_l(t)$ is:

$$I_l(0) = [T \sum_{n=-\infty}^{\infty} d_l g(nT - \tau_l)] [\sum_{i=0}^{N-1} \cos(i\omega_d \tau_l + \phi_{IF} + \theta_i^{l0})]. \quad (2.15)$$

where d_l is a discrete random variable uniformly distributed on $\{1, -1\}$, and ϕ_{IF} is a random variable uniformly distributed on $(0, 2\pi)$. τ_l , the relative delay of user l with respect to user 0, is also a random variable uniformly distributed on $(-\infty, \infty)$. Since the correlation window of a matched filter is finite, the range for τ_l could be considered the length of that window, and the result be averaged over a large number of such windows, instead of assuming $(-\infty, \infty)$ range which has the same effect. These random variables are mutually independent.

Since $\overline{d_l} = 0$, it can be easily concluded that:

$$\overline{I_l} = 0$$

and as it is shown in Appendix C:

$$\overline{I_l^2} = \frac{N}{2} T^2 (1 - \frac{\alpha}{4}). \quad (2.16)$$

From equation (2.4) the signal power is obtained as:

$$\begin{aligned} \overline{D^2} &= \frac{N^2}{4} \sum_{i=-\infty}^{\infty} T^2 g^2(t - iT) \\ &= \frac{N^2}{4} T^2 \end{aligned} \quad (2.17)$$

Equation (2.17) shows that the desired signal power at the output is proportional to N^2 whereas by equation (2.16) the co-user interference is proportional to N . Therefore, the larger the N , the larger the signal to co-user interference ratio. It is

also important to note that, co-user interference in this case is independent of users' phase sequence choices regardless of pulse shape.

In a FS-SS CDMA system when there are $(M - 1)$ co-users transmitting, the interferences caused by each of them at the desired receiver are independent, and therefore the total interference power is $P_I = (M - 1)\overline{I_I^2}$. In fact as M increases, by the central limit theorem, this interference becomes a close approximation of Gaussian noise.

2.5.2 Overlap FS-SS

When $W < \omega_d < 2W$, neighboring subbands overlap and co-users cause an additional interference, compared to the non-overlap FS-SS. As in the previous section, co-user signal is despread by $q_0(t)$ and passed through the matched filter. Using equation (2.9), the co-user signal at the matched filter output can be written as:

$$\begin{aligned} J_i(t) &= \{[s_i(t) * h(t)]q_0(t)\} * p(t) \\ &= M_i(t) + O_i(t) \end{aligned} \tag{2.18}$$

where $M_i(t)$ is the main lobe signal and $O_i(t)$ is the tail signal. $J_i(T_0)$ is the co-user error added to the decision variable at the sampling time T_0 .

As it is shown in Appendix C, the mean value of $J_i(T_0)$ is 0, i.e.,

$$\overline{J_i(T_0)} = 0$$

The variance of $J_i(T_0)$ has three components:

$$\overline{J_i^2(T_0)} = \overline{M_i^2(T_0)} + \overline{O_i^2(T_0)} + 2\overline{O_i(T_0)M_i(T_0)}. \tag{2.19}$$

These three components are calculated in Appendix C. The first one is the same as $\overline{I_i^2(T_0)}$ except for $\omega_d = 1/T$:

$$\overline{M_i^2(T_0)} = \frac{N}{2} z_1(0) + \text{Re}\{z_1(1) \sum_{i=1}^{N-1} \cos(\theta_i^{0i} - \theta_{i-1}^{0i})\} \quad (2.20)$$

where $z_1(0)$ and $z_1(1)$ are parameters independent of users' phase sequences, obtained in Appendix C. For a proper choice of phase sequences (Chapter 3), the summation term in equation (2.20) is small, and since $z_1(0)$ does not depend on sampling instance T_0 , equation (2.20) can be simplified as:

$$\overline{M_i^2(T_0)} = \frac{N}{2} z_1(0)$$

The second term in equation (2.19) is:

$$\overline{O_i^2(T_0)} = (N - 1) z_3(0)$$

where $z_3(0)$ is defined in Appendix C, and also is independent of T_0 and users' phase sequences. The third component has the form:

$$\overline{M_i(T_0)O_i(T_0)} = 2\text{Re}\{z_4(0) \sum_{i=1}^{N-1} \exp[j(\theta_i^0 - \theta_{i-1}^0)] + z_4(-1) \sum_{i=1}^{N-1} \exp[j(\theta_i^1 - \theta_{i-1}^1)]\} \quad (2.21)$$

where $|z_4(0)|$ and $|z_4(-1)|$ do not change with the choice of T_0 . This component is small when the phase sequence Θ^1 and Θ^0 are chosen properly. Tables 2.1, 2.2, 2.3, 2.4 list $z_1(0)$, $|z_1(1)|$, $z_3(0)$, $|z_4(0)|$ and $|z_4(-1)|$, for different overlap coefficients(η), and some values of α , namely $\alpha = 0.35$, $\alpha = 0.5$, $\alpha = 0.65$ and $\alpha = 1$, respectively. These results show how f_d may be chosen to minimize co-user interference power.

Also using coset codes, introduced in Chapter 3, causes interference terms including $z_1(1)$, $z_4(0)$ and $z_4(1)$ to be small.

f_d	η	$z_1(0)/T^2$	$ z_1(1) /T^2$	$z_3(0)/T^2$	$ z_4(0) /T^2$	$ z_4(-1) /T^2$
$1.35/2T$	0.5	0.9125	0	0.3250	0.3463	0
$1.5/2T$	0.44	0.9125	0	0.2501	0.2714	0
$1.75/2T$	0.35	0.9125	0	0.1341	0.1511	0
$2/2T$	0.26	0.9125	0.0438	0.0437	0.0557	0.0557
$2.25/2T$	0.17	0.9125	0	0.0064	0.0089	0
$2.5/2T$	0.07	0.9125	0	0.0001	0.0002	0
$2.7/2T$	0	0.9125	0	0.0000	0.0000	0

Table 2.1: OFS-SS co-user interference components for $\alpha = 0.35$

f_d	η	$z_1(0)/T^2$	$ z_1(1) /T^2$	$z_3(0)/T^2$	$ z_4(0) /T^2$	$ z_4(-1) /T^2$
$1.5/2T$	0.5	0.8750	0	0.2528	0.2826	0
$1.75/2T$	0.42	0.8750	0	0.1434	0.1695	0
$1.85/2T$	0.38	0.8750	0	0.1068	0.1299	0
$2/2T$	0.33	0.8750	0.0625	0.0625	0.0796	0.0796
$2.25/2T$	0.25	0.8750	0	0.0184	0.0250	0
$2.5/2T$	0.17	0.8750	0	0.0028	0.0040	0
$2.75/2T$	0.08	0.8750	0	0.0001	0.0001	0
$3/2T$	0	0.8750	0	0.0000	0.0000	0

Table 2.2: OFS-SS co-user interference components for $\alpha = 0.5$

f_d	η	$z_1(0)/T^2$	$ z_1(1) /T^2$	$z_3(0)/T^2$	$ z_4(0) /T^2$	$ z_4(-1) /T^2$
$1.65/2T$	0.5	0.8375	0	0.1963	0.2308	0
$1.8/2T$	0.45	0.8375	0	0.1406	0.1708	0
$2/2T$	0.39	0.8375	0.0813	0.0812	0.1034	0.1034
$2.2/2T$	0.33	0.8375	0	0.0406	0.0539	0
$2.4/2T$	0.26	0.8375	0	0.0167	0.0231	0
$2.6/2T$	0.21	0.8375	0	0.0052	0.0074	0
$2.8/2T$	0.15	0.8375	0	0.0010	0.0015	0
$3.3/2T$	0	0.8375	0	0.0000	0.0000	0

Table 2.3: OFS-SS co-user interference components for $\alpha = 0.65$

f_d	η	$z_1(0)/T^2$	$ z_1(1) /T^2$	$z_3(0)/T^2$	$ z_4(0) /T^2$	$ z_4(-1) /T^2$
$2/2T$	0.5	0.7500	0.1250	0.1250	0.1591	0.1591
$2.25/2T$	0.44	0.7500	0	0.0720	0.0950	0
$2.5/2T$	0.38	0.7500	0	0.0368	0.0502	0
$2.75/2T$	0.33	0.7500	0	0.0161	0.0225	0
$3/2T$	0.25	0.7500	0	0.0056	0.0081	0
$3.25/2T$	0.19	0.7500	0	0.0014	0.0021	0
$3.5/2T$	0.13	0.7500	0	0.0001	0.0003	0
$4/2T$	0	0.7500	0	0.0000	0.0000	0

Table 2.4: OFS-SS co-user interference components for $\alpha = 1$

Let us obtain the number of users a FS-SS CDMA system can accommodate in different situations (capacity of the system) , assuming an acceptable level of performance. Setting a bit error rate of 10^{-3} and noting that data modulation is PSK and coherent detection is used, PSK bit error rate curve versus SNR can be used to find the respective SNR [18] which is 7db. To be able to make comparisons, we assume the total bandwidth in any case is the same, and compare the capacities. Using the results obtained before, one may write the following expression for SNR:

$$\text{SNR} = \frac{T^2 N^2 / 4}{(M - 1)[(N/2)z_1(0) + (N - 1)z_3(0)]} \quad (2.22)$$

In equation (2.22) co-users' interference components which depend on the phase sequences are ignored, assuming a proper choice of phase sequences in the system.

Let us assume the total available bandwidth is the amount sufficient for non-overlapping FS-SS and $\alpha = 0.35$ with $N_0 = 63$, then $N = N_0$ and the required bandwidth is:

$$B_0 = 63\left(\frac{1.35}{T}\right)$$

For non-overlap case $N \neq N_0$. Using equation (2.14) the number of subbands needed

to fit OFS-SS signal spectrum in B_0 is approximately:

$$N = \frac{B_0}{f_d} = \frac{(63)(1.35)}{f_d T}$$

Letting $\text{SNR} = 10^{0.7} = 5$ and substituting N into equation (2.22) , M , the maximum number of users, is obtainable. Figure 2.9 shows the graph of the number of users supported by FS-SS CDMA system in this example for different values of α and f_d .

Figure 2.9 shows some properties of FS-SS. In non-overlapping FS-SS ($\eta = 0$) for larger values of α , the number of users is smaller, as it is expected, because the number of subbands (N) is smaller. Also, for each value of α capacity is larger when overlap is allowed. This suggest that the advantage of spectrum saving in OFS-SS outweigh the disadvantage of additional interference due to overlap.

In DS-SS, a rule of thumb for the SNR of a CDMA system, with M_{ds} users, is [15]:

$$\text{SNR} = \left[\frac{M_{ds} - 1}{3N_{ds}} + \frac{N_n}{2E} \right]^{-1/2} \quad (2.23)$$

where $\frac{E}{N_n}$ is the signal to thermal noise power ratio and N_{ds} is spreading ratio (SR) defined as:

$$N_{ds} = \frac{B_{SS}}{B_{data}}$$

where B_{SS} is the bandwidth of the spread spectrum signal and B_{data} is the double sided data signal bandwidth. Ignoring thermal noise and using the same SNR chosen as before, the number of users M_{ds} is obtained by:

$$M_{ds} = (5^{-2})(3N_{ds}) + 1 = 0.12N_{ds} + 1$$

Table 2.5.2 shows the values of M_{ds} for spreading ratios used for FS-SS in last example. Spreading ratio for any α is the number of subbands in non-overlapping

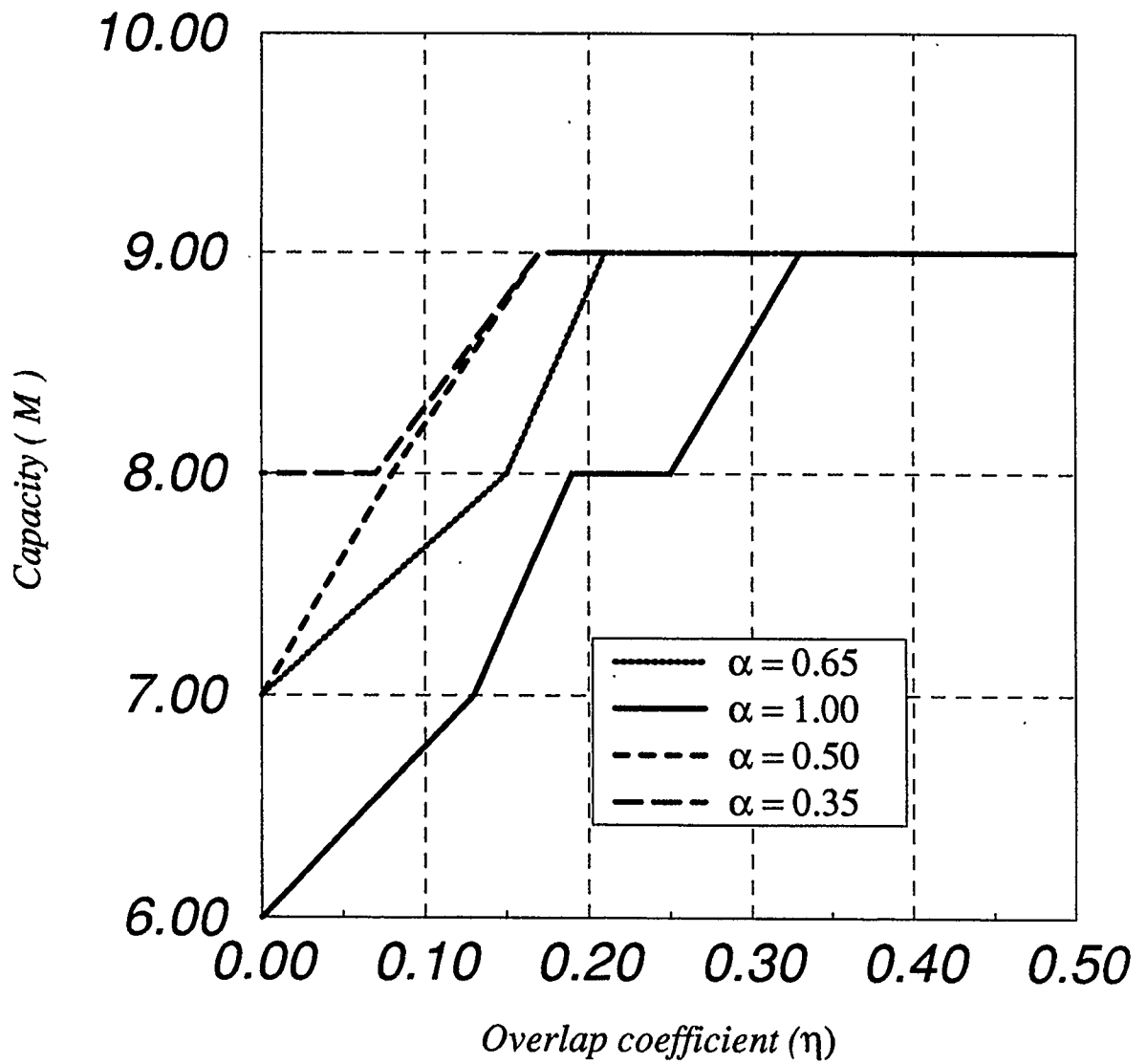


Figure 2.9: Capacity of a FS-SS CDMA using SRRC signaling versus overlapping coefficient η for different values of α .

α	Spreading Ratio(N_{ds})	DS-SS Capacity (M_{ds})	non-overlapping FS-SS Capacity (M)
0.35	63	8	8
0.50	57	7	7
0.65	52	7	7
1	43	6	6

Table 2.5: DS-SS and FS-SS capacity comparison

FS-SS. Comparing the the results with the graphs in Figure 2.9, one may note that the capacity of DS-SS system is close to the non-overlapping FS-SS ($\eta = 0$), and therefore a relative improvement in capacity is achievable using OFS-SS.

Manipulating equations (2.23) and (2.22) results in the following equations for capacities of DS-SS and FS-SS systems:

$$M_{ds} - 1 = \frac{1}{\text{SNR}^2}(3N_{ds}) \quad (2.24)$$

$$M_{fs} - 1 = \frac{T^2 N^2 / 4}{\text{SNR}[(N/2)z_1(0) + (N - 1)z_3(0)]} \quad (2.25)$$

Comaring equations (2.24) and (2.25), one may note that $(M_{ds} - 1)$ is proportional to $1/\text{SNR}^2$, whereas $(M_{fs} - 1)$ is proportional to $1/\text{SNR}$. This means that in a system with lower bit error rate, where higher SNR is required, the capacity of DS-SS system decreases faster that the capacity of FS-SS system.

Chapter 3

Code Design

3.1 Introduction

In Chapter 2 the mechanism of spreading and despreading using FS-SS was explained and it was shown that co-users' interference powers do not depend on the choice of their phase sequences in non-overlapping FS-SS. Although for OFS-SS there is a term in the co-user interference powers that depends on the choices of codes, for most phase sequences considered, that term is small. However, the peaks of co-user interferences depend on the factor $AIX(\phi)$ in equation (2.8), which in turn is a function of phase sequences assigned to each user. Minimizing $AIX(\phi)$ is essential in fast synchronization acquisition, which is one of the performance indexes of a CDMA system [19]. Therefore, it is quite important to minimize these interferences by finding proper phase sequences.

The focus in this chapter is to find such sets of sequences. At first, some observa-

tions about the behavior of AIX factor is mentioned and then some sets of sequences are investigated.

3.2 Definitions and Observations

Definition 3.1 *We define a function CR as:*

$$CR(\phi, \Theta) = \left| \sum_{i=0}^{N-1} \exp(i\phi + \theta_i) \right| \quad (3.1)$$

where $\Theta = \theta_0\theta_1 \dots \theta_{N-1}$ is a sequence of phases and therefore:

$$AIX = CR(\phi_d, \Theta^{kl})$$

If sequence $\Theta^{kl} = \Theta^k - \Theta^l$ is known, AIX is only a function of ϕ which represents the delay. In fact, there is a mapping from Θ^{kl} onto the function $AIX_{kl}(\phi)$ which is equivalent to cross-correlation function in DS-SS. In comparison AIX_{kl} can be called “cosine cross-correlation of sequences Θ^k and Θ^l ”.

One can make the following observations which are quite important in the search for good codes.

Observation 3.1 *The phase sequence Θ^k in equation (2.2) is, in fact, the characteristic sequence of user k . Let us limit the number of possible values of θ_i^k in the range $(0, 2\pi)$ to L , namely the set $F[L] = \{0, 2\pi/L, 2(2\pi/L), \dots, (L-1)(2\pi/L)\}$ which can be mapped onto set $C[L] = \{0, 1, 2, \dots, L-1\}$. $\{c_i = \theta_i(L/2\pi) \in C[L], i = 0, \dots, N-1\}$ is a sequence which we call code sequence. Sum or difference of any two elements in $F[L]$ after subtracting multiples of 2π from it, is again in $F[L]$. The equivalent operation in $C[L]$ is addition modulo L and $C[L]$ is closed under this*

operation:

$$\text{if } c_i \in C[L], c_j \in C[L] \quad \text{then } c_i \pm c_j \in C[L] \quad (3.2)$$

Since $c_i \in C[L]$ for $i = 0, \dots, N - 1$ the sequence $C = c_0 c_1 \dots c_{N-1}$ belongs to $C^N[L]$, the set of all N -tuples with elements in $C(L)$, and if we define summation and subtraction of sequences as:

$$C^k \pm C^l = \{c_i^k \pm c_i^l \pmod{L} \quad i = 0, \dots, N - 1\}$$

then $C^N[L]$ is closed under these operations. From now on by $+$ or $-$ operations for code sequences we mean addition or subtraction as is defined above.

Definition 3.2 If C is a code sequence in $C^N[L]$ we define R as:

$$R(\phi, C) = CR(\phi, (2\pi/L)C) \quad (3.3)$$

Observation 3.2 Assume Θ is a phase sequence in $F^N[L]$, the set of all N -tuples with element in $F(L)$. If there is any $\psi \in F[L]$ and positive integer $N_1 < N$ such that:

$$\theta_{i+N_1} = \theta_i + \psi \quad i = 0, \dots, N_2$$

where $N_1 < N_2 < N - N_1 + 1$, then there may be some large peaks in $CR(\phi, \Theta)$ for $\phi = \frac{2K\pi - \psi}{N_1}$, $K = 1, 2, \dots, N_1$ (Appendix B) and the peaks are the largest when $N_2 = N - 1$.

This fact suggest that there should not be any incremental pattern in the phase sequence.

One case which may occur in some sequences and should be avoided, is when $\psi = 0$. In this case there is a repetitive phase pattern of length N_1 in the sequence.

Figure 3.1 shows two example of such cases. In Figure 3.1a there are some peaks occurring at $\phi = [(2K - 1)\pi]/10$, and in Figure 3.1b the peaks occur at $\phi = 2K\pi/8$.

To visualize the behavior of CR function, any exponential in equation (3.1) can be considered as a unit vector and CR is the sum of them. For $\phi = 0$, these vectors stretch along $0, 2\pi/L, 2(2\pi/L), \dots, (L - 1)(2\pi/L)$ directions and they start rotating counterclockwise with different speeds around the unit circle as ϕ increases. A good code is the one that guarantees distribution of vectors around the unit circle as uniformly as possible for all values of $\phi \in (0, 2\pi)$. Intuitively, if vectors are distributed randomly in different direction, a good uniformity of distribution can be expected for all ϕ s. Figure 3.2 illustrates this representation.

3.3 Pseudorandom Sequences

In FS-SS CDMA system a sequence is assigned to each user, namely Θ^k to user k , $k = 1, \dots, M$. These sequences should be selected such that $CR(\phi, \Theta^{kl})$ for $k, l = 1, \dots, M$ $k \neq l$ are as low as possible for all $\phi \in (0, 2\pi)$. One method could be finding good Θ^{kl} sequences and then going back to design the Θ^k s. In general, this approach does not work because designed Θ^k s may generate some Θ^{kl} s which are not in the original set. However, since sum or difference of any two elements in a group are in the same group, if Θ^{kl} s are chosen to form a group, then Θ^k s can be chosen from that group.

Two properties of forming a group and randomness of phases in a sequence suggest that a class of sequences called 'maximal length sequences' could be a candidate in FS-SS too. Some of the manipulations that will be performed on the code sequences

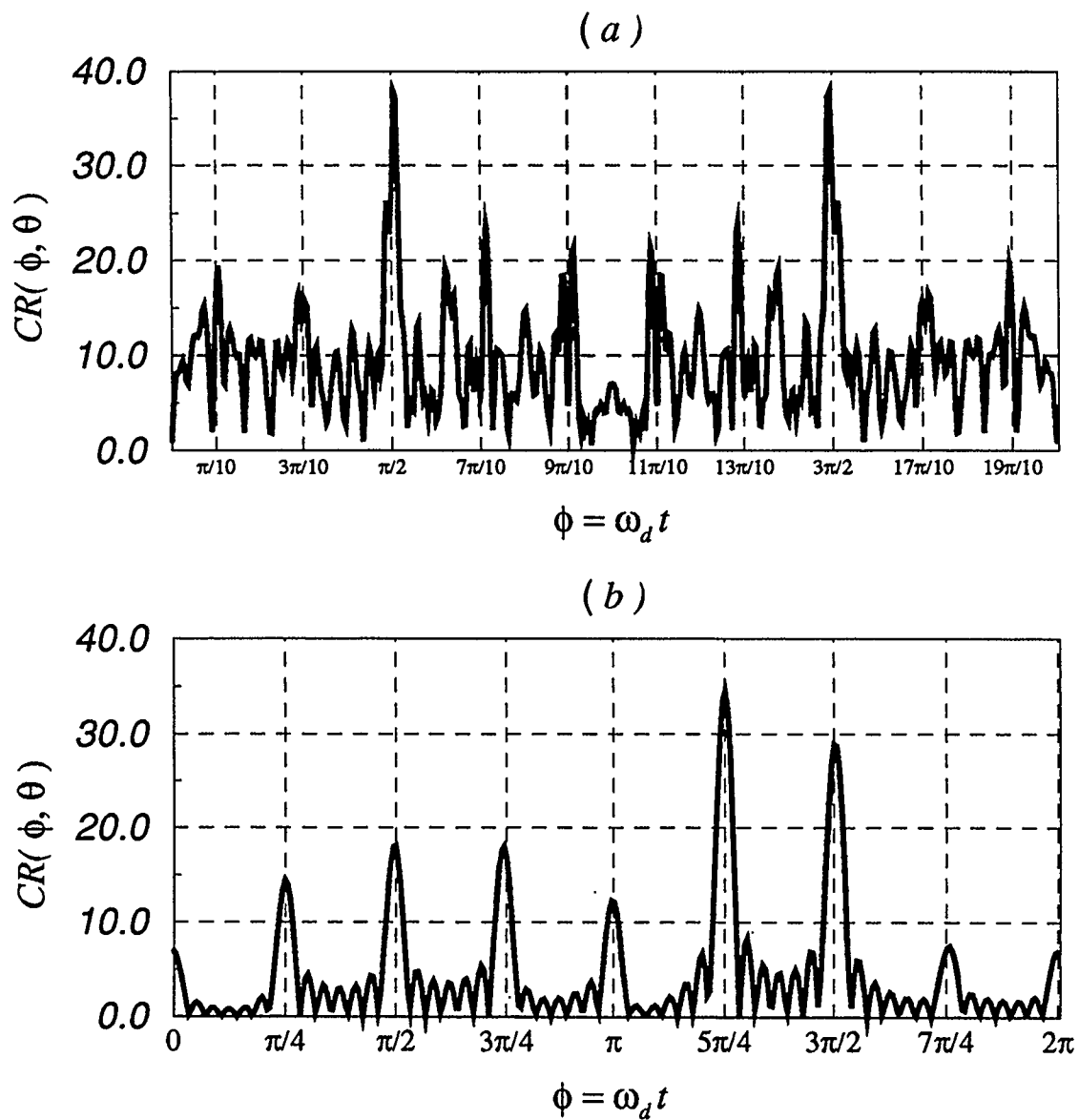


Figure 3.1: Effect of incremental patterns in phase sequences on cosine cross-correlation: a) $N = 127, N_1 = 10, N_2 = 52, \psi = \pi, L = 2$ b) $N = 56, N_1 = 8, N_2 = 49, \psi = 0, L = 3$.

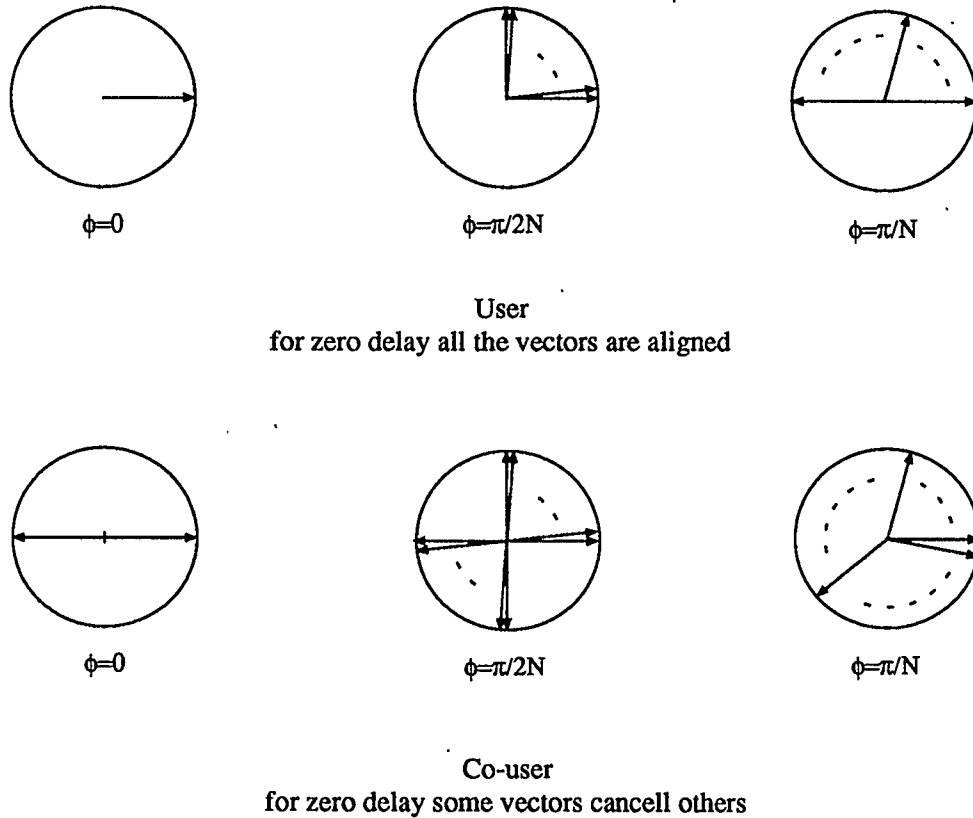


Figure 3.2: Vector representation of cosine cross-correlation behavior.

require an understanding of the mechanics of finite fields. it seems necessary to review briefly what are needed in designing the code sequences.

3.3.1 Groups

A group G is a set of objects [20], or elements, for which an operation is defined, and for which Axioms 1 to 4 hold. Let g_1, g_2, g_3, \dots , be elements of the group. The operation is a single-valued function of two variables which is customarily denoted by $a + b = c$ or $ab = c$ and called addition or multiplication, even though it may not be the addition or multiplication of ordinary numbers.

Axiom 1 (Closure). *The operation can be applied to any two group elements to give a third element as a result.*

Axiom 2 (Associative Law). *For any three elements g_i, g_j and g_l of the group, $(g_i + g_j) + g_l = g_i + (g_j + g_l)$ if the operation is written as addition, $(g_i g_j) g_l = g_i (g_j g_l)$ if the operation is written as multiplication.*

The associative law means that the order of performing operations is not important, and so parentheses are unnecessary.

Axiom 3 (Identity element). *There is an identity element $e \in G$.*

If the operation is called addition, the identity element is called zero and written 0 and is defined by the equation $0 + g_i = g_i + 0 = g_i$ for any $g_i \in G$. If the operation is called multiplication, the identity is one, written 1, and defined by the equation $1g_i = g_i1 = g_i$.

Axiom 4 (Inverse element). *Every element of a group has an inverse element.*

If the operation is addition, the inverse of element g_i is denoted by $-g_i$ and defined by the equation $g_i + (-g_i) = (-g_i) + g_i = 0$. If the operation is multiplication, the inverse of g_i is denoted by g_i^{-1} and defined by the equation $g_i g_i^{-1} = g_i^{-1} g_i = 1$.

In addition to the above laws, a group may satisfy the commutative law; that is, $g_i + g_j = g_j + g_i$ or $g_i g_j = g_j g_i$ if the operation is multiplication. Such a group is called *Abelian* or *commutative*.

For developing some properties of groups the multiplicative notation is used hereafter.

Theorem 3.1 *The identity in a group is unique, and the inverse of each group element is also unique.*

Examples. The set of all real numbers is a group under ordinary addition. The set of all positive and negative integers and zero is also a group under addition. All these groups are abelian. The set of all nonsingular $n \times n$ matrices is a non-abelian group, under the operation matrix multiplication.

Subgroups and Factor Groups

A subset of elements of a group G is called a subgroup H if it satisfies all the axioms for the group itself with the same operation. To determine whether H is a subgroup, it is necessary to check only for closure (that is, if a and b are in H , then ab must be in H) and for inverses (that is, if a is in H , then a^{-1} must be also). If a set is closed under the group operation and the inverse is present, identity must be present also, and associative law holds in the subgroup if it does in the group.

Suppose that the elements of a group G are g_1, g_2, g_3, \dots , and the elements of a subgroup H are h_1, h_2, h_3, \dots , and consider the array formed as follows: The first row is the subgroup, with the identity at the left and each other element appearing once and only once. The first element in the second row is any element not appearing in the first row, and the rest of elements are obtained by multiplying each subgroup element by this first element on the left. Similarly a third, fourth, and fifth row are formed, each with a previously unused group element in the first column, until all

the group elements appear somewhere in the array.

$$\begin{array}{cccccccc}
 h_1 & = & 1, & & h_2, & & h_3, & & h_4, & \dots, & & h_n \\
 g_1 h_1 & = & g_1, & & g_1 h_2, & & g_1 h_3, & & g_1 h_4, & \dots, & & g_1 h_n \\
 g_2 h_1 & = & g_2, & & g_2 h_2, & & g_2 h_3, & & g_2 h_4, & \dots, & & g_2 h_n \\
 \vdots & & & & \vdots & & \vdots & & \vdots & & \vdots & \vdots \\
 g_m h_1 & = & g_m, & & g_m h_2, & & g_m h_3, & & g_m h_4, & \dots, & & g_m h_n
 \end{array}$$

The set of elements in a row of this array is called a *left coset*, and the element appearing in the first column is called the *coset leader*. Right cosets could be similarly formed. The array itself is known as the *coset decomposition* of the group.

Theorem 3.2 *Two elements g and g' of a group G are in the same left coset of a subgroup H of G if and only if $g^{-1}g'$ is an element of H .*

Theorem 3.3 *Every element of the group G is in one and only one coset of a subgroup H .*

A subgroup H of a group G is called *normal* if, for any element h of H and any element g of G , $g^{-1}hg$ is in H . In such a case it is possible to define an operation on cosets to form a new group for which cosets are the elements. This group is called the *factor group* and denoted by G/H . The coset containing g is denoted $\{g\}$. The definition of multiplication for cosets is

$$\{g_1\}\{g_2\} = \{g_1g_2\}$$

This definition is possible because, no matter which element is chosen as a representative of each of the two cosets to be multiplied, the resulting coset is the same. It

can be shown that if g_1 and g'_1 are in the same coset, and g_2 and g'_2 are in the same coset, then g_1g_2 and $g'_1g'_2$ are also in the same coset.

3.3.2 Rings

A *ring* is a set of elements for which two operations are defined. One is called addition and denoted $a + b$, and the other is called multiplication and denoted ab , even though these operations may not be ordinary addition or multiplication of numbers. In order for R to be a ring, the following axioms must be satisfied:

Axiom 5 *The set R is an Abelian group under addition.*

Axiom 6 (Closure). *For any two elements a and b of R , the product ab is defined and is an element of R .*

Axiom 7 (Associative law). *For any three elements a , b , and c of R , $a(bc) = (ab)c$.*

Axiom 8 (Distributive law). *For any three elements a , b , and c of R , $a(b + c) = ab + ac$ and $(b + c)a = ba + ca$.*

A ring is called *commutative* if its multiplication operation is commutative; that is, $ab = ba$ for any $a, b \in R$.

Theorem 3.4 *In any ring, for any element a and b , $a0 = 0a = 0$ and $a(-b) = (-a)b = -ab$.*

Examples. The set of all real numbers is a commutative ring under the operations of ordinary addition and multiplication. The set of all polynomials in one variable, with integer coefficients is another example of a commutative ring.

3.3.3 Fields

A field is a commutative ring with a unit element (multiplicative identity) in which every nonzero element has a multiplicative inverse.

Note that the nonzero elements of a field satisfy all the axioms for a group and form a group under the operation multiplication.

Examples. The set of all real numbers form, a field, as do also the set of all rational numbers and the set of all complex numbers.

It can be shown that for every number q that is a power of a prime number there is a finite field with q elements. However, it might be well to point out here that a field with p elements can be formed by taking the integers modulo p ($F(p)$), provided p is a prime. $F(p)$ is a Galois fields.

Let us define $f(x) = f_n x^n + f_{n-1} x^{n-1} + \dots + f_0$ as a polynomial of degree n over field F when the coefficients f_n, f_{n-1}, \dots, f_0 are in F . A polynomial $h(x)$ over the field $F(p)$ is called *irreducible* if, no $g(x)$ of degree less than n , divides it. A polynomial $h(x)$ of degree n is said to be *primitive* if the smallest integer q for which $h(x)$ divides $x^q - 1$ is $q = p^n - 1$. It can be shown that the set of polynomials over $F(p)$ form a finite field with p^n elements under the multiplication operation defined as ordinary multiplication of polynomials modulus irreducible polynomial $h(x)$ of degree n . This field is known as Galois field $GP(p^n)$.

3.3.4 Maximal Length Sequences

Maximal length sequences (m-sequences) are an important class of sequences in some applications such as DS-SS for constructing sets of low cross-correlation codes. The

properties of these sequences and also shift register circuits for generating them have been investigated in a number of references [21] [1]. Since m-sequences seem to be proper choice in FS-SS, in this section their generation and some of their related properties are reviewed.

Let n be a positive integer, and let a_0, \dots, a_{k-1} be given elements of a finite field $F(p)$. A sequence s_0, s_1, \dots of elements in $F(p)$ satisfying the relation

$$s_{n+k} = a_{k-1}s_{n+k-1} + a_{k-2}s_{n+k-2} + \dots + a_0s_n \quad (3.4)$$

is called a (*kth-order*) *linear recurring sequence* over $F(p)$. The terms s_0, s_1, \dots, s_{k-1} , which determine the rest of sequence uniquely, are referred to as the initial values. The polynomial

$$f(x) = x^k - a_{k-1}x^{k-1} - a_{k-2}x^{k-2} - \dots - a_0$$

is called the *characteristic polynomial* of the linear recurring sequence.

It can be shown that if $f(x)$ is a primitive polynomial then sequence s_0, s_1, \dots is periodic with the period $q = p^n - 1$. One period of this sequence ($s = s_0, s_1, \dots, s_q$) is called maximal length sequence.

For any primitive polynomial $f(x)$ there are q different initial values and therefore q different m-sequences, which form a set of sequences $S[f]$. These m-sequences could be shown to be shifted versions of each other and $S[f] = \{s, T^1s, T^2s, \dots, T^{q-1}s\}$ where T^i denotes an operator which shifts vectors cyclicly to the left by i places. In the course of generation of an m-sequence, the vector s_{n+k-1}, \dots, s_n will take all possible *k-tuples* with elements in $F(p)$.

One of the properties of m-sequences is that in these sequences, the elements of underlying finite field appear about equally often in the full period and also in large

segments of the full period [21]. Also, the appearance of these elements throughout the sequence follows a pseudo-random pattern. These properties make m-sequences appealing for FS-SS.

Another point about m-sequences is that, for a primitive polynomial $f(x)$, $S_0[f] = \{S[f], 0\}$ forms a group under the addition operation defined as

$$s + t = s_0 + t_0, s_1 + t_1, \dots, s_q + t_q.$$

Since $S[f]$ is a subset of the group of all the possible sequences of length q over the finite field $F(p)$, it only remains to show closure and existence of inverse elements in $S[f]$.

Let us assume s^1 and s^2 in $S[f]$ is generated by two different initial conditions s_0^1, \dots, s_{n-1}^1 and s_0^2, \dots, s_{n-1}^2 . Using equation (3.4) one can write:

$$\begin{aligned} s_n^1 + s_n^2 &= (a_{n-1}s_{n-1}^1 + \dots + a_0s_0^1) + (a_{n-1}s_{n-1}^2 + \dots + a_0s_0^2) \\ &= a_{n-1}(s_{n-1}^1 + s_{n-1}^2) + \dots + a_0(s_0^1 + s_0^2) \end{aligned}$$

which means $s^1 + s^2$ is the sequence generated by initial value $s_0^1 + s_0^2, \dots, s_{n-1}^1 + s_{n-1}^2$ and the same polynomial $f(x)$; therefore it is in $S[f]$. Consequently, it can be seen that the inverse of s^1 is another sequence generated by the initial value $-s_{n-1}^1, \dots, -s_0^1$.

3.4 Code Performances

In this section the performance of some codes are investigated in both overlap and non-overlap FS-SS. For non-overlap FS-SS, maximum of $R(\phi, C)$ is chosen as an index of performance, where $C = C^i - C^j$ is a sequence resulting from subtraction

of user i and j 's code sequences. Sequences of length $p^n - 1$ are considered for some values of p and n where p is a prime number.

3.4.1 Non-overlap FS-SS Codes

Let us consider an example of binary m-sequence set with characteristic polynomial

$$f(x) = x^5 + 0x^4 + x^3 + x^2 + x^1 + 1 \quad (3.5)$$

and initial value 10000; then $s = 1000010110101000111011111001001$ is the generated m-sequence. Figure 3.3 shows $R(\phi, s)$ in terms of ϕ and Figure 3.4 illustrates $\max[R(\phi, T^i s)]$ for $i = 0, \dots, q - 1$.

In Figure 3.3, it can be seen that although the highest peak is 9.64, the frequency of occurrence is low and for most delays the bound $R(\phi, s)$ is less than 7. This scenario is typical for most sequences in FS-SS. Figure 3.4 shows that $\max[R(\phi, s)]$ can be as high as 11.2 for some $s \in S[f]$, but there are also sequences with highest peak of cosine cross-correlation of 8. For the same spreading ratio in DS-SS, and almost the same number of sequences, Gold codes seem to be a good choice which has maximum cross-correlation peak (MCP) of 9 for all pairs of the sequences in the set. This suggest that this m-sequence in FS-SS may perform comparably with Gold codes in DS-SS.

The highest and lowest cosine cross-correlation peaks in the m-sequence sets $S[f]$ for different primitive polynomials $f(x)$ over finite fields $F(p)$ are listed in tables 3.1, 3.2, 3.3, 3.5, 3.6, respectively, for $p = 2$, $p = 3$, $p = 5$ and $p = 7$. In these tables the polynomial $a_0x^n + a_1x^{n-1} + \dots + a_n$ is abbreviated in the form $a_0a_1 \dots a_n$ with $a_0 = 1$. The left-hand column, headed by the value of n , lists primitive polynomials

f for degree n and the modulus p concerned.

The point to be noted is that the second highest peak (AP_2) in the cosine auto-correlation which depends solely on sequence length, is smaller than its equivalent in DS-SS for $N < 63$ and this peak occurs only for one value of time delay.

In a FS-SS system a set of m-sequences can be chosen and each sequence in the set assigned to a user. By doing this we have made sure that $s^{kl} = s^k - s^l$ is in the same set and the maximum and minimum of $\max[R(\phi, s^{kl})]$ are found from tables 3.1, 3.3, 3.5 and 3.6.

Let us define a factor λ as:

$$\lambda_{FS-SS} = \frac{N}{MCCP}$$

where N is the sequence length and an indicator of desired user signal level when synchronization is obtained, and $MCCP$ is the mean cosine cross-correlation peak which is the average of $\max[R(\phi, s)]$ values for $s \in S[f]$. An equivalent factor could be introduced in DS-SS as $\lambda_{DS-SS} = N/(MCP)$ where MCP is maximum cross-correlation peak (using Gold codes). If the partial cross-correlations are taken into account in DS-SS, the λ s in both cases are comparable.

3.4.2 Overlap FS-SS Codes

In the last section, classes of sequences for non-overlap FS-SS were introduced. The principles which were applied there, would be utilized for codes in OFS-SS. As it was pointed out in the first chapter, after despreading and low pass filtering (or matched filtering), the resulting signal consists of two components: the main lobe and the tail signal.

Polynomial coefficient	$\max[\max R(\phi, s)]$	$\min[\max R(\phi, s)]$	Average of Peaks	AP_2	
$n = 3, (N = 7)$					
1011	5	3.1	4	1.6	
1101	5	3.1	4		
$n = 4, (N = 15)$					
10011	7.2	5.5	6.4	3.3	
11001	7.2	5.5	6.4		
$n = 5, (N = 31)$					
100101	11.1	8.6	9.8	6.8	
101001	11.1	8.6	9.8		
101111	11.2	8	9.8		
111101	11.2	8	9.8		
110111	13	8.4	9.8		
111011	13	8.2	9.7		
$n = 6, (N = 63)$					
1000011	16.4	11.9	14.2		13.7
1011011	16.2	12	13.9		
1100001	16.4	11.9	14.2		
1100111	17.5	11.6	14.2		
1101101	16.2	12	13.9		
1110011	17.5	11.6	14.2		
$n = 7, (N = 127)$					
10000011	24.1	18.1	20.8	27.5	
10001001	25.1	17.5	20.7		
10001111	24.4	18.3	20.9		
10010001	25.1	17.5	20.7		
10011101	24.3	18.3	20.9		
10100111	25	18.4	20.8		
10101011	24.2	18.4	20.7		
10111001	24.3	18.3	20.9		
10111111	24	18	20.8		

Table 3.1: Maxima and minima of peak cosine auto- and cross-correlations for m-sequences for $p = 2$

Polynomial coefficient	$\max[\max R(\phi, s)]$	$\min[\max R(\phi, s)]$	Average of Peaks	AP_2
$n = 7, (N = 127)$ (Cont'd)				
11000001	24.1	18.1	20.8	
11001011	24	18	20.7	
11010011	24	18	20.7	
11010101	24.2	18.4	20.7	
11100101	25	18.4	20.8	
11101111	25	18.4	20.9	
11110001	24.4	18.3	20.9	
11110111	25	18.4	20.9	
11111101	24	18	20.7	
$n = 8, (N = 255)$				
100011101	36.5	26.8	30.2	52.7
100101011	34.7	26.7	30.3	
100101101	39	27.3	30.7	
101001101	34.7	26.9	30.3	
101011111	35	26.5	30.2	
101100011	36.1	27.1	30.3	
101100101	34.7	26.9	30.3	
101101001	39	27.3	30.7	
101110001	36.5	26.8	30.2	
110000111	36.1	27.1	30.3	
110001101	36.1	26.6	30.3	
110101001	34.7	26.7	30.3	
111000011	36.1	27.1	30.3	
111001111	35.7	26.3	30.2	
111100111	35.7	26.3	30.2	
111110101	35	26.5	30.2	

Table 3.2: (Table 3.1, Cont'd), Maxima and minima of peak cosine auto- and cross-correlations for m-sequences for $p = 2$

Polynomial coefficient	$\max[\max R(\phi, s)]$	$\min[\max R(\phi, s)]$	Average of Peaks	AP_2
$n = 2, (N = 8)$				
112	5.4	4.1	4.7	1.8
122	5.4	4.1	4.7	
$n = 3, (N = 26)$				
1021	10.6	8	9.1	5.7
1121	10.3	7.7	9.2	
1201	10.6	8	9.1	
1211	10.3	7.7	9.2	
$n = 4, (N = 80)$				
10012	19.2	14.8	16.7	17.4
10022	19	15.5	17	
11002	19	15.5	17	
11122	19.9	14.9	16.7	
11222	19.9	14.9	16.7	
12002	19.2	14.8	16.7	
12112	20.4	15.5	17.4	
12212	20.4	15.5	17.4	
$n = 5, (N = 242)$				
100021	34.2	26.6	30.1	52.5
100211	34.4	27.4	30.8	
101011	33.1	27	30.3	
101201	36.3	27.2	30.3	
101221	35.7	28	30.7	
102101	36.3	27.2	30.3	
102211	35	27.3	30.6	
110021	34	27.6	30.8	
110101	33.1	27	30.3	
110111	34.7	27.2	30.2	
111011	34.7	27.2	30.2	
111121	34.5	27.7	30.6	
111211	36.8	27.6	30.9	
112001	33.4	27.8	30.8	

Table 3.3: Maxima and minima of peak cosine auto- and cross-correlations for m-sequences for $p = 3$

Polynomial coefficient	$\max[\max R(\phi, s)]$	$\min[\max R(\phi, s)]$	Average of Peaks	AP_2
$n = 5, (N = 242), (Cont'd)$				
112111	36.8	27.6	30.9	
112201	35	27.3	30.6	
120001	34.2	27	30.1	
120011	34	27.6	30.8	
120221	33.3	27.7	30.6	
121111	34.6	27.7	30.6	
122021	33.3	27.7	30.6	
122101	35.7	28	30.7	

Table 3.4: (Table 3.3, Cont'd) Maxima and minima of peak cosine auto- and cross-correlations for m-sequences for $p = 3$

The main lobe behaves as if it is non-overlap FS-SS, and is proportional to $R(\phi, s^{lk})$ where $s^{lk} = s^l - s^k$. The tail signal is weighted by the factor Z in equation (2.13).

With a closer look at equation (2.13), one can distinguish two parts, each similar to the factor $R(\phi, s)$. The difference is that now the code sequences are $u^{lk_1} = u^l - T^1 u^k$ and $u^{k_1 l} = u^k - T^1 u^l$ with length $N - 1$. For large N the effect of shorter length is negligible and $i = 0$ can be included in the summation terms in equation (2.13). Therefore $T(\phi, u^k, u^l)$ is simplified as:

$$\begin{aligned}
Z(\phi, u^k, u^l) &= \left| \sum_{i=0}^{N-1} \exp[j(\frac{2\pi}{p}(u_i^k - u_{i-1}^l) + (i-1)\phi)] \right| \\
&\quad + \left| \sum_{i=0}^{N-1} \exp[j(\frac{2\pi}{p}(u_{i-1}^k - u_i^l) + i\phi)] \right| \\
&= \left| \exp(-j\phi) \sum_{i=0}^{N-1} \exp[j(\frac{2\pi}{p}(u_i^k - u_{i-1}^l) + i\phi)] \right| \quad (3.6) \\
&\quad + \left| \sum_{i=0}^{N-1} \exp[j(\frac{2\pi}{p}(u_{i-1}^k - u_i^l) + i\phi)] \right| \\
&= R(\phi, u^{k_1 l}) + R(\phi, u^{l_1 k}).
\end{aligned}$$

Let us assume that sequences for different users are chosen from a set of m-sequences, i.e. $u^k \in S[f]$ for $k = 1, \dots, M$. In this case, the effective sequences u^{lk_1} and $u^{l_1 k}$,

Polynomial coefficient	$\max[\max R(\phi, s)]$	$\min[\max R(\phi, s)]$	Average of Peaks	AP_2
$n = 2, (N = 24)$				
112	10	7.6	8.7	5.2
123	9.7	7.6	8.6	
133	10	7.6	8.7	
142	9.7	7.6	8.6	
$n = 3, (N = 124)$				
1032	24.4	18.7	21.3	26.5
1033	25	19.2	21.4	
1042	24.8	18.5	21.5	
1043	23.9	18.6	21.0	
1102	25	19.2	21.1	
1113	24	19	21.2	
1143	24.5	18	21.3	
1203	24.8	18.5	21.5	
1213	23.9	19.1	21.0	
1222	24	19	21.2	
1223	25.6	18.7	21.5	
1242	23.9	19.1	21.0	
1302	23.9	18.6	21.0	
1312	24.9	18.5	21.5	
1322	24.5	18	21.3	
1323	24.7	17.9	21.2	
1343	24.9	18.5	21.5	
1403	24.4	18.7	21.3	
1412	24.7	17.9	21.2	
1442	25.6	18.7	21.5	

Table 3.5: Maxima and minima of peak cosine auto- and cross-correlations for m-sequences for $p = 5$

Polynomial coefficient	$\max[\max R(\phi, s)]$	$\min[\max R(\phi, s)]$	Average of Peaks	AP_2
$n = 2, (N = 48)$				
113	15.2	11.5	12.8	10.4
123	14.7	11.3	12.7	
125	14.8	10.9	12.7	
145	14.4	11.5	12.6	
153	14.4	11.4	12.6	
155	15.2	11.5	12.8	
163	14.8	10.9	12.7	
$n = 3, (N = 342)$				
1032	43.7	32.9	37.4	72.8
1052	41.9	32.1	37.0	
1062	41.1	33.2	36.6	
1112	39.3	32.6	36.4	
1124	42.4	33.6	37.5	
1152	42.8	32.2	37.1	
1154	42.3	32.8	36.9	
1214	41.5	32.6	36.9	
1242	41.5	32.6	37.0	
1262	43.7	33.4	36.8	
1264	39.9	33.1	36.3	
1304	40.9	32.8	36.4	
1314	43.7	33.4	36.8	
1322	42.3	32.8	36.9	
1334	41.9	34.2	37.1	
1352	42.2	32.9	37.5	
1354	44.1	33.8	36.9	
1362	44.1	33.8	36.9	
1422	42.4	33.9	37.5	
1432	41.3	32.9	36.3	
1434	42.5	33.5	36.6	
1444	39.4	33	36.3	

Table 3.6: Maxima and minima of peak cosine auto- and cross-correlations for m-sequences for $p = 7$

Polynomial coefficient	$\max[\max R(\phi, s)]$	$\min[\max R(\phi, s)]$	Average of Peaks	AP_2
$n = 3, (N = 342)$				
1504	45.6	33.6	37.5	
1524	41.3	32.9	36.3	
1532	40	33.5	36.5	
1534	42.9	32.7	37.3	
1542	39.9	33	36.3	
1552	42.2	33.4	36.5	
1564	40	33.5	36.5	
1604	42.1	33.2	36.9	
1612	42.5	33.5	36.6	
1632	42.9	32.7	37.3	
1644	42.4	32	36.7	
1654	42.2	32.9	37.5	
1662	42.9	34.2	37	
1664	42.2	33.4	37	

Table 3.7: (Table 3.6, Cont'd) Maxima and minima of peak cosine auto- and cross-correlations for m-sequences for $p = 7$

are also in $S[f]$, which means some lower bounds for factor Z are guaranteed. There is an exception for $u^k = T^1 u^l$ or $u^l = T^1 u^k$ which causes u^{lk_1} or $u^{l_1 k}$ to be 0. In such a situation some large peaks of $Z(\phi_d)$ will appear for $\phi = 2K\pi$ (K is an integer). Depending on the amount of adjacent subbands overlap, this may or may not be tolerable because at $\phi = 2K\pi$, $R(\phi, s^{kl})$ (the main lobe weight) is very small. From above one can conjecture that for small overlaps m-sequences still are good choices.

If large peaks of $Z(\phi_d)$ are intolerable, the m-sequences assigned to each user should be such that $s^k \neq T^1 s^l$ for any two users k and l . This condition limits the number of users the system can support to almost a half:

$$\{s, T^2 s, T^4 s, \dots, T^r s\}$$

where $r = (N + 1)/2$ for $p = 2$ and $r = N/2$ for $p \neq 2$. The solution to this problem

lies in the idea of cosets.

Cosets of m-sequences

It was shown that the set of m-sequences $S_0[f]$ form a subgroup of M_N , the group of all vectors with length $N = p^n - 1$ and elements in the finite field $F(p)$. Let us form a coset of this subgroup by adding an arbitrary non-zero vector $t \in M_N - S[f]$ to all the m-sequences in $S[f]$ and call it $S[f, t]$:

$$\text{if } s \in S[f] \text{ then } u = s + t \in S[f, t].$$

It can be observed that u^{kl} is still in $S[f]$:

$$u^{kl} = u^k - u^l = (s^k + t) - (s^l + t) = s^k - s^l = s^{kl} \in S[f]$$

This means that regardless of the choice of t , the sequences of the cosets provide the system with good weight factor peaks for the main lobe.

The situation is different for tail signal weight factor Z . Sequences u^{kl_1} and u^{k_1l} can be written as:

$$\begin{aligned} u^{kl_1} &= u^k - T^1 u^l = (s^k + t) - (T^1 s^l + T^1 t) = (s^k - T^1 s^l) + (t - T^1 t). \\ u^{k_1l} &= T^1 u^k - u^l = (T^1 s^k + T^1 t) - (s^l + t) = (T^1 s^k - s^l) + (T^1 t - t). \end{aligned} \quad (3.7)$$

The sequences $(s^k - T^1 s^l)$ and $(T^1 s^k - s^l)$ are elements of $S_0[f]$, therefore if $tt^1 = t - T^1 t$ and $t^1 t = T^1 t - t$, then u^{kl_1} and u^{k_1l} are in the cosets $S[f, tt^1]$ and $S[f, t^1 t]$ respectively.

Coset Selection

In the previous subsection, it was shown that if the users' codes are chosen from a coset $S[f, t]$, then the weight factor of the main lobe will be the same as the case

when the codes are in $S[f]$. Now the question is how to pick a sequence t , to obtain minimum peaks for $T(\phi, u^k, u^l)$.

To obtain the peaks of $T(\phi, u^k, u^l)$ for $u^k, u^l \in S[f, t]$, N^2 times $\max[T(\phi, u^k, u^l)]$ should be calculated for $k, l = 0, \dots, N-1$. An alternative approach, which reduces the amount of calculations, is to find a sequence t which provides reasonably small peaks for $R(\phi, u^k - Tu^l)$ and $R(\phi, u^l - Tu^k)$. It can easily be shown:

$$\begin{aligned} R(\phi, u^k - Tu^l) &= R[\phi, (s^k - Ts^l) + tt^1] \\ R(\phi, u^l - Tu^k) &= R[\phi, (s^l - Ts^k) + t^1t] \\ tt^1 &= -t^1t \\ s^k - Ts^l, s^l - Ts^k &\in S_0[f] \end{aligned}$$

Lemma 3.1 *For any sequence s :*

$$\max[R(\phi, -s)] = \max[R(\phi, s)]$$

for $\phi \in [0, 2\pi]$. *The proof is in Appendix B.*

Let us proceed with choosing a sequence v and calculate $\max[R(\phi, s + v)]$ for $s \in S_0[f]$ and call the highest one R_m . By Lemma 3.1 and noting that $S_0[f]$ forms a group, R_m is also the highest peak of $R(\phi, s - v)$:

$$\max R(\phi, s - v) = \max R(\phi, -s + v) \quad -s \in \{S[f] + 0\}$$

Therefore, the problem of finding a sequence t to minimize the highest peak of $T(\phi, u^k, u^l)$ reduces to searching for a v which minimizes the largest maximum of $R(\phi, s + v)$ for $s \in S_0[f]$, where $v = tt^1$. Sequence t can be obtained by noting:

$$v = t - Tt \rightarrow t_i = v_i + t_{i-1}, \quad i = 1, \dots, N-1 \quad (3.8)$$

Now, by choosing an initial value for t_0 , the rest of the sequence is obtained from equation (3.8). For $i = N$, t_N may not be the same as t_0 , which is not a critical issue, because the original sequences in $T(\phi, u^k, u^l)$ have $N - 1$ element.

For minimizing the peaks of $R(\phi, s+v)$, randomness of $s+v$ is a factor. Therefore, a natural choice is to select v from another m-sequence set. In fact trying many sequences as v for different N suggests that phases of some m-sequences are proper choices.

Figures 3.5, 3.6, 3.7, 3.8, show the highest and lowest peaks, and the mean of $\max[R(\phi, s + T^i v)]$ for $s \in S[f]$ versus i , when v is also an m-sequence generated by $g(x)$ and initial condition vi_0 for different values of N . In these figures f and g represent coefficients of $f(x)$ and $g(x)$, respectively.

3.5 Conclusion

In this Chapter Some classes of code sequences were studied in terms of their performance in minimizing the peaks of the co-users' main lobe and tail signal weight factors. Maximal length sequences and their cosets were investigated as proper choices of code sequences for FS-SS and OFS-SS. FS-SS CDMA system designer can use Tables 3.1, 3.3, 3.5, 3.6 to choose a suitable set of sequences for his specific system. For example if the number of users are small, some sequences of a set that has lower minimum peak, may be preferable.

Figures 3.5, 3.6, 3.7, 3.8 show maxima, minima, and mean of the peaks of tail signal weight factor for some m-sequence cosets in OFS-SS. Since in all the figures the mean and minimum of the peaks do not change significantly from one set to another,

Sequence Length	Correlation Peak
31	9
63	17
127	17
255	33 (Gold-like sequences)

Table 3.8: Cross-correlation peaks of Gold codes in DS-SS

one may choose the set that provide the smallest maximum peak. For example, in Figure 3.7, the set obtained for $i = 41$, is a good choice.

In DS-SS, auto- and cross-correlations have almost the same role as cosine auto- and cross-correlations in FS-SS. Table 3.5 lists some auto- and cross-correlation maxima for Gold codes [14]. Comparing these peaks with the numbers in Table 3.1, one may notice that maximum of auto- and cross-correlation of Gold codes are smaller than maximum peaks and very close to the average peak in non-overlapping FS-SS. When system is asynchronous, the peaks of co-user interference in DS-SS depend on odd auto- and cross-correlations of the sequences [14] which are typically larger than periodic auto- and cross-correlation, whereas in FS-SS cosine auto- and cross-correlations do not depend on the data and in the cases such as PSK modulation in any subbands, the co-user interference peaks will be smaller.

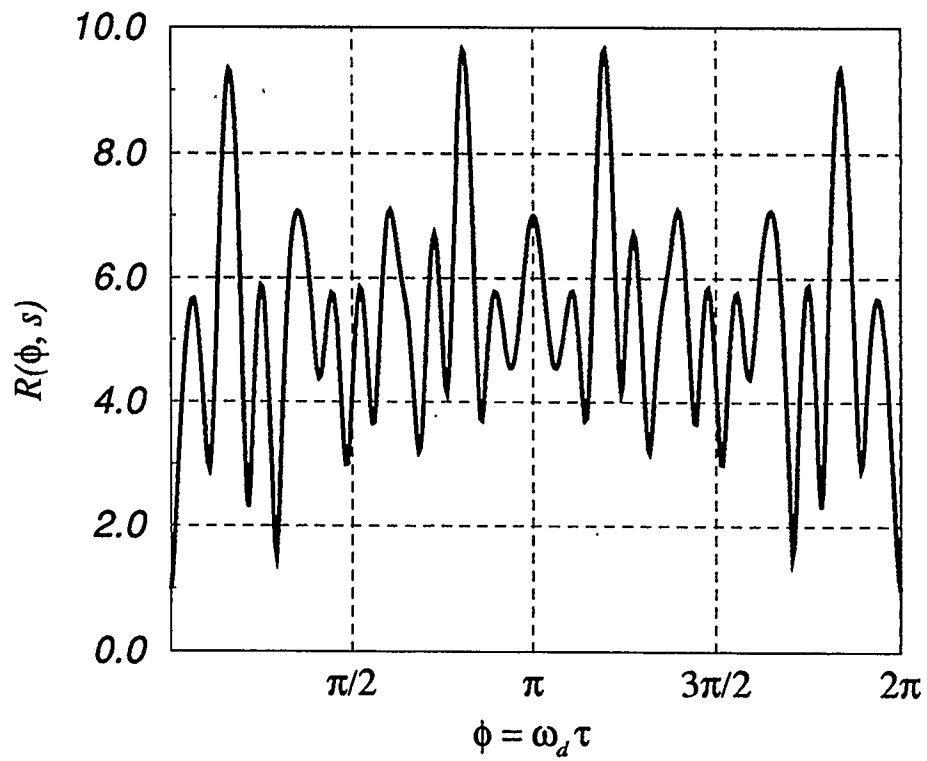


Figure 3.3: $R(\phi, s)$ versus $\phi = \omega_d \tau$ for a typical m-sequence s , generated by $f(x)$ in equation (3.5) and initial value 10000.

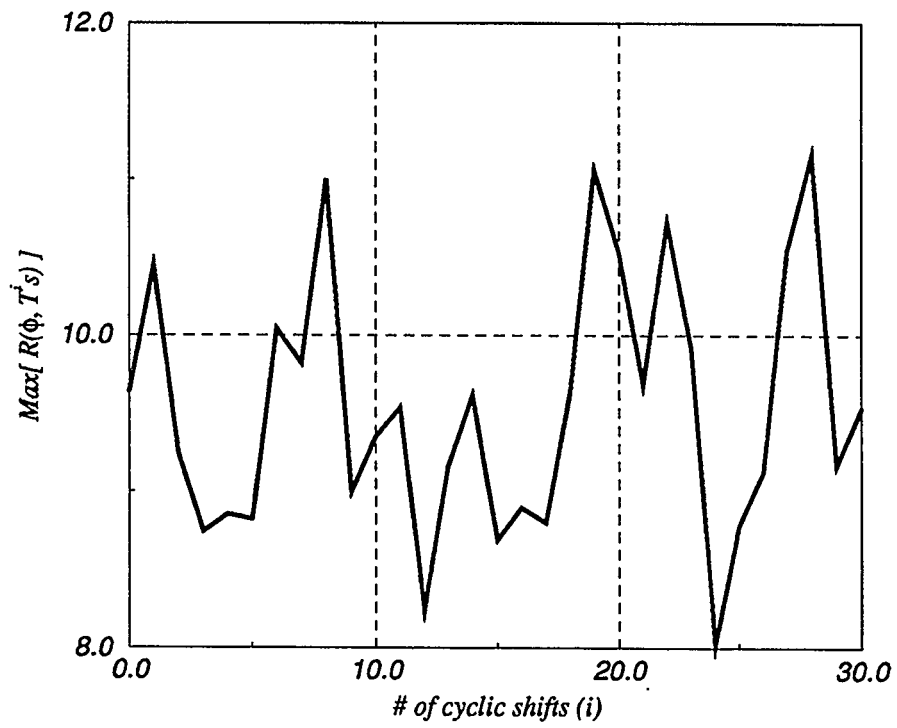


Figure 3.4: $\max(R(\phi, T^i s))$ for set $S[f]$ generated by $f(x)$ in equation (3.5)

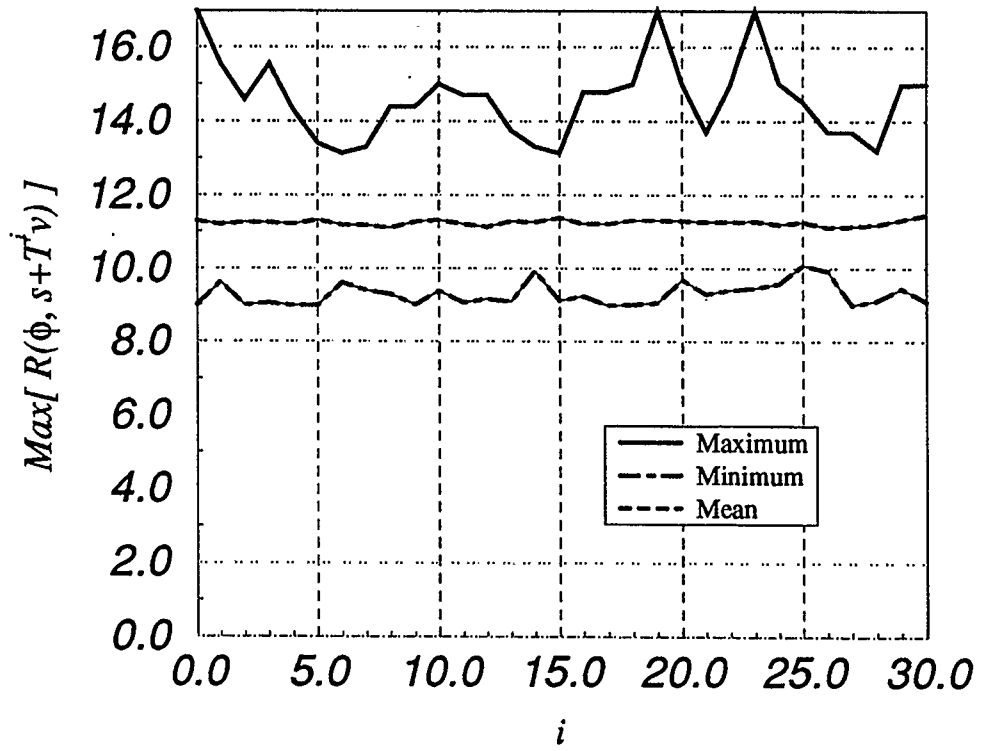


Figure 3.5: Cosine cross-correlation peaks for coset generated by $f = 101111$, and $g = 111101$, $v_{i_0} = 10000$. $N = 31$

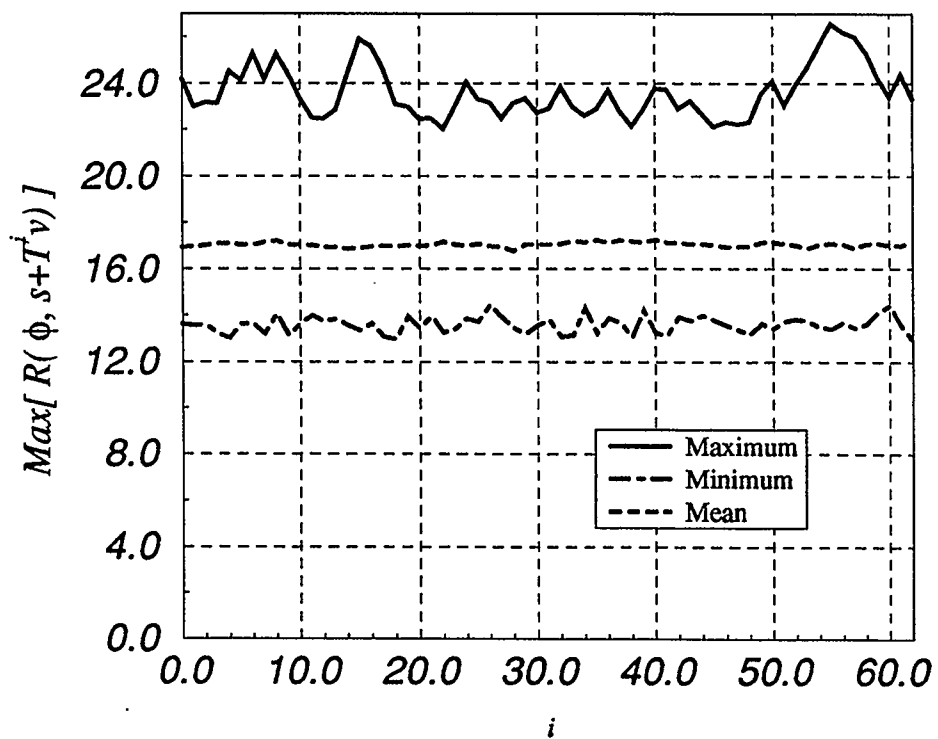


Figure 3.6: Cosine cross-correlation peaks for coset generated by $f = 1100001$, and $g = 1110011$, $v_i_0 = 100000$. $N = 63$

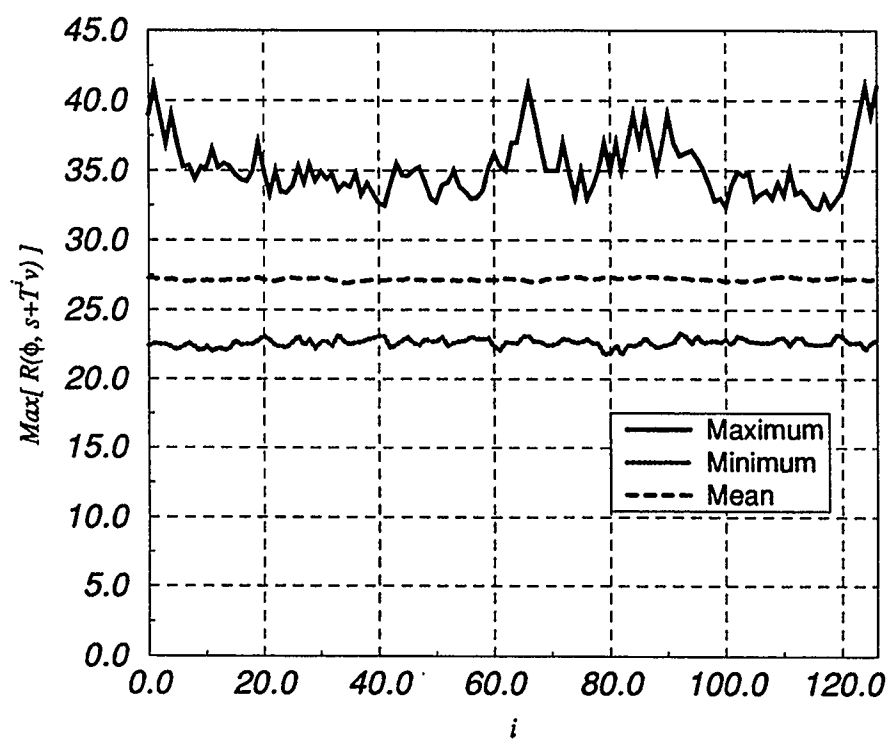


Figure 3.7: Cosine cross-correlation peaks for coset generated by $f = 11000001$, and $g = 10111111$, $v_{i_0} = 1000000$. $N = 127$

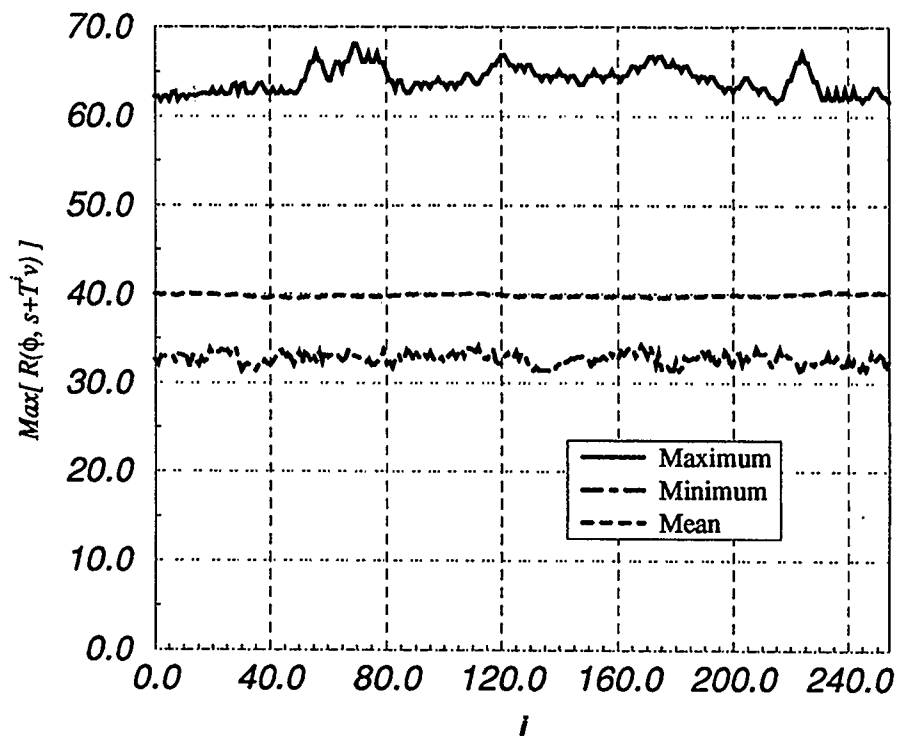


Figure 3.8: Cosine cross-correlation peaks for coset generated by $f = 101110001$, and $g = 101011111$, $v_i_0 = 10000000$. $N = 255$

Chapter 4

Conclusions

The main purpose of this thesis was to investigate a new spread spectrum technique, namely frequency sequence spread spectrum (FS-SS), with emphasis on its characteristics, such as co-user interferences, in CDMA applications.

FS-SS uses a sequence of subcarriers, located equidistantly in the frequency domain, as spreading signal. The amplitude of these impulses are equal and their phases follow a unique sequence for each user. Modulating the information signal with this signal, generates a spread spectrum signal which is a repetition of the data signal in a sequence of subbands, with a phase offset by the subcarrier phase in that frequency slot. Despreading is accomplished by demodulating FS-SS signal using a synchronized replica of spreading signal and low pass filtering the result.

Two variations of this technique have been considered: non-overlapping FS-SS where no two adjacent subbands overlap, and overlapping FS-SS (OFS-SS) in

which neighboring subbands are allowed to overlap. Although OFS-SS requires less RF bandwidth, it produces more co-user interference in CDMA applications than FS-SS.

4.1 Spreading Mechanism Comparison

Two widely used spread spectrum techniques are direct-sequence (DS) and frequency-hopping (FH) spread spectrum. Major differences between DS-SS and FS-SS spreading mechanisms are as follow:

1. Spreading parameters are controlled in the time domain for DS-SS, whereas in FS-SS these parameters are designed in frequency domain.
2. The spectrum of spreading waveform for DS-SS is a sequence of impulses, but unlike FS-SS the amplitudes and phases of these impulses is a function of chip waveform, and therefore can have any value.
3. In DS-SS the desired receiver, having the knowledge of spreading waveform, is able to align all the chips in the data symbol period and add them up to obtain a strong signal; whereas co-user chips remain distributed in different directions and the summation during a symbol interval is small. In FS-SS this alignment is meaningful in the frequency domain. The desired receiver is able to align all the subbands and add them up at baseband to recover the original signal, but the co-user signals remain unaligned when translated to baseband.

Frequency-hopping spread spectrum also uses different subcarriers to spread the information signal, but in this scheme transmission is narrowband at any given time, whereas FS-SS uses all the subcarriers simultaneously.

4.2 Co-user Interferences

In a SS-CDMA system, all the users transmit simultaneously on the same frequency band, and therefore, each co-user causes an error in the decision variable at the sampling time at the receiver. Since transmissions are considered asynchronous, these errors are independent.

Analysis showed that, in non-overlapping FS-SS, the mean of each co-user interference is zero and its power is independent of the phase sequence choices for users. In the case of overlapping FS-SS, there are additional terms in the co-user interference power, one of which is dependent on the co-user phase sequence. For many choices of phase sequence sets (e.g. maximal length sequences), when N (number of subbands) is large, this term is negligible. This is in contrast to DS-SS, where each co-user interference depends on the users' code sequences [15].

4.3 Phase Sequences

Although the phase sequence choices for users, is not of primary concern in co-user interference power, they are important in minimizing the instantaneous peaks of co-user signals. If these peaks are large, the synchronization time can be quite long which can degrade the performance of the system, considerably. A class of sequences, known as maximal length sequences, which are widely used for code design in DS-SS, offer good performance in terms of peak cosine cross-correlation. Cosine cross-correlation is an indicator of co-user signal level for any delay between despreading waveform and co-user signal. These peaks are comparable with cross-correlation peaks of Gold sequences in DS-SS.

In overlapping FS-SS, a co-user signal at the receiver has two components: the main lobe signal which is the same as non-overlapping FS-SS, and the tail signal which is a result of subbands overlapping. In this case, depending on the overlap depth and system requirement, m-sequences may not perform satisfactorily because large peaks of tail signals are expected. Some alternative sequences which are cosets of m-sequences have been introduced and investigated. These sequences provide the same peaks for the main lobe signal as m-sequences, but smaller peaks for the tail signals.

4.4 Suggestions For Future Work

FS-SS is a new spread spectrum technique, and should be investigated in many respects to find out its advantages in different applications. In a practical system, implementation is an important factor. FS-SS can be implemented by analog or digital circuits, and the merits of each one need to be investigated. Also, synchronization techniques for FS-SS, is another area of research. Other pulse shapes, and phase sequences that may provide better performance should be searched for. Performance evaluation of FS-SS combined with coding and other spread spectrum schemes, are fields of further research too. Other types of channels, for example multipath, should also be investigated.

Bibliography

- [1] Rodger E. Ziemer and Rodger L. Peterson, *Digital Communications and Spread Spectrum Systems*, Macmillan Publishing Company, 1985.
- [2] Raymond L. Pickholtz, Donald L. Schilling, and Laurance B. Milstein, "Theory of spread spectrum communications - a Tutorial", *IEEE Transaction on Communications*, vol. Com-30, pp. 855-884, May 1982.
- [3] Donald L. Schilling, Laurance B. Milstein, et al., "Spread spectrum for commercial communications", *IEEE Communications Magazine*, vol. , pp. 66-79, April 1991.
- [4] Robert A. Scholtz, "The origins of spread spectrum communications", *IEEE Transaction on Communications*, vol. COM-30, pp. 822-854, May 1982.
- [5] Marlin P. Ristenbatt and James L. Daws, Jr., "Performance criteria for spread spectrum communications", *IEEE Transaction on Communications*, pp. 756-763, August 1977.
- [6] George L. Turin, "Introduction to spread spectrum antimultipath techniques and their application to urban digital radio", *Proceedings of the IEEE*, vol. 68, pp. 328-353, March 1980.
- [7] Audrey M. Viterbi and Andrew J. Viterbi, "Erlang capacity of a power controlled cdma system", *IEEE Journal on Selected Areas on Communications*, vol. 11, pp. 892-900, August 1993.

- [8] Klein S. Gilhousen et al., "On the capacity of a cellular CDMA system", *IEEE Transaction on Vehicular Technology*, vol. 40, pp. 303–312, May 1991.
- [9] Peter Jung and Walter Baier, "Advantage of CDMA and spread spectrum techniques over FDMA and TDMA in cellular mobile radio applications", *IEEE Transaction on Vehicular Technology*, vol. 42, pp. 313–322, August 1993.
- [10] William C. Y. Lee, "Overview of cellular CDMA", *IEEE Transaction on Vehicular Technology*, vol. 40, pp. 291–302, May 1991.
- [11] R.Lupas and S.verdu, "Near-far resistance of multiuser detectors in asynchronous channels", *IEEE Transaction on Communications*, vol. 38, pp. 496–508, April 1990.
- [12] Robert A. Scholtz, "The spread spectrum concept", *IEEE Transaction on Communications*, vol. COM-25, pp. 748–755, August 1977.
- [13] Mohsen Kavehrad and George E Bodeep, "Design and experimental results for a direct-sequence spread-spectrum radio using differential phase-shift keying modulation for indoor, wireless communications", *IEEE Journal on Selected Areas on Communications*, vol. SAC-5, pp. 815–823, June 1987.
- [14] Dilip V. Sarwate and Michael Pursley, "Crosscorrelation properties of pseudo-random and related sequences", *Proceedings of the IEEE*, vol. 68, pp. 593–619, May 1980.
- [15] Michael B.Pursley, "Performance evaluation for phase-coded spread-spectrum multiple-access communications part i: System analysis", *IEEE Transaction on*

- Communications*, vol. COM-25, pp. 795–799, August 1977.
- [16] Serdar Boztas, Rodger Hammons, and Vijay Kumar, “4-phase sequences with near-optimum correlation properties”, *IEEE Transaction on Information Theory*, vol. 38, pp. 1101–1113, May 1992.
- [17] Sandeep Chennakeshu and G. J. Saulnier, “Differential detection of $\pi/4$ -shifted DQPSK for digital cellular radio”, in *IEEE Conference on Vehicular Technology*, pp. 186–191, 1991.
- [18] K. Sam Shanmugam, *Digital and Analog Communication Systems*, John Wiley & Sons, Inc., 1979.
- [19] Upamanyu Madhow and Michael B. Pursley, “Acquisition in direct-sequence spread spectrum communication networks: An asymptotic analysis”, *IEEE Transaction on Information Theory*, vol. 39, pp. 903–912, May 1993.
- [20] W. Wesley Peterson and E. J. Weldon, Jr., *Error-Correcting Codes*, The MIT Press, 1972.
- [21] Rudolf Lidl and Harald Niederreiter, *Introduction to Finite Fields and Their Applications*, Cambridge University Press, 1986.

Appendix A

Cosine Auto-correlation

A.1 Cosine Auto-correlation Formula

Equation (2.7) is established using the following analysis:

$$\begin{aligned} AMX(x) &= \left| \sum_0^{N-1} \exp[j(ix)] \right| = \frac{\sin(x/2)}{\sin(x/2)} \left| \sum_0^{N-1} \exp[j(ix)] \right| \\ &= \left| \frac{1}{2 \sin(x/2)} \sum_{i=0}^{N-1} \{ \exp[j(ix + x/2)] - \exp[j(ix - x/2)] \} \right| \\ &= \left| \frac{\exp[j((N-1)x + x/2)] - \exp[j(-x/2)]}{2 \sin(x/2)} \right| \\ &= \left| \frac{\exp[j(Nx/2 - x/2)] \{ \exp[j(Nx/2)] - \exp[j(-Nx/2)] \}}{2 \sin(x/2)} \right| \\ &= \left| \frac{\sin(Nx/2)}{\sin(x/2)} \right| \end{aligned}$$

A.2 Cosine Auto-correlation Peaks

Using equation 2.6, cosine auto-correlation function is:

$$AMX(\phi) = \left| \sum_{i=0}^{N-1} \exp[j(i\phi)] \right|$$

An example of this function for $N = 31$ is shown in Figure 2.4. Using the vector analogy used in Section 3.2, one may note that $AMX(\phi)$ is the amplitude of summation of N vectors. when $\phi = 0$, all these vectors are aligned and the first and the highest peak in Figure 2.4 results. As ϕ increases, these vectors start rotating counterclockwise with different speeds, but any two subsequent vectors maintain a phase difference of ϕ . Figure A.1 show this vector representstion for the sequence length $N = 8$. For a ϕ close to $2\pi/N$, these vectors cancell out each other almost

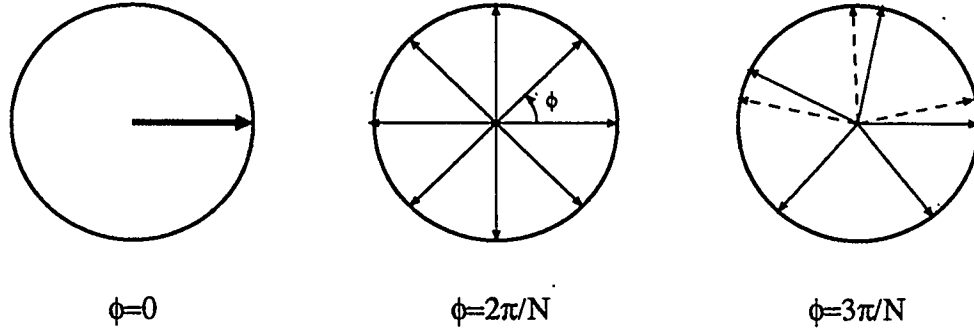


Figure A.1: Vector representation of cosine auto-correlation.

totally, and the first null in Figure A.2 is produced. As ϕ continues to increase, the vectors distributed in the range $(0, 2\pi)$ still cancel out each other and the ones which have passed 2π line, start to build up a non-zero vector. For $\phi = \frac{3\pi}{N}$, second peak in Figure A.2 is resulted, and when ϕ increases more, the vectors passing line 3π , cancel some vectors in the upper semicircle; therefore reducing the amplitude of $AMX(\phi)$.

Using the same line of reasoning, it can be concluded that the peaks of $AMX(\phi)$ happen at some phases close to $\frac{(2m+1)\pi}{N}$, and therefore m -th cosine auto-correlation peak is ($m \neq 0$):

$$AP_m = \left| \frac{\sin\left[\frac{N}{2}\left(\frac{(2m+1)\pi}{N}\right)\right]}{\sin\left[\frac{(2m+1)\pi}{2N}\right]} \right|$$

and since $\sin(x) \simeq x$ for $x < 0.5$ with an error less than 2%, one can obtain the following result:

$$\begin{aligned} AP_m &= \left| \frac{\sin\left[\frac{(2m+1)\pi}{2}\right]}{\frac{(2m+1)\pi}{2N}} \right| \\ &= \frac{2N}{(2m+1)\pi} \end{aligned}$$

for

$$\frac{(2m+1)\pi}{2N} < 0.5 \quad \longrightarrow \quad m/N < 1/(2\pi)$$

$$\text{or } m < N/6$$

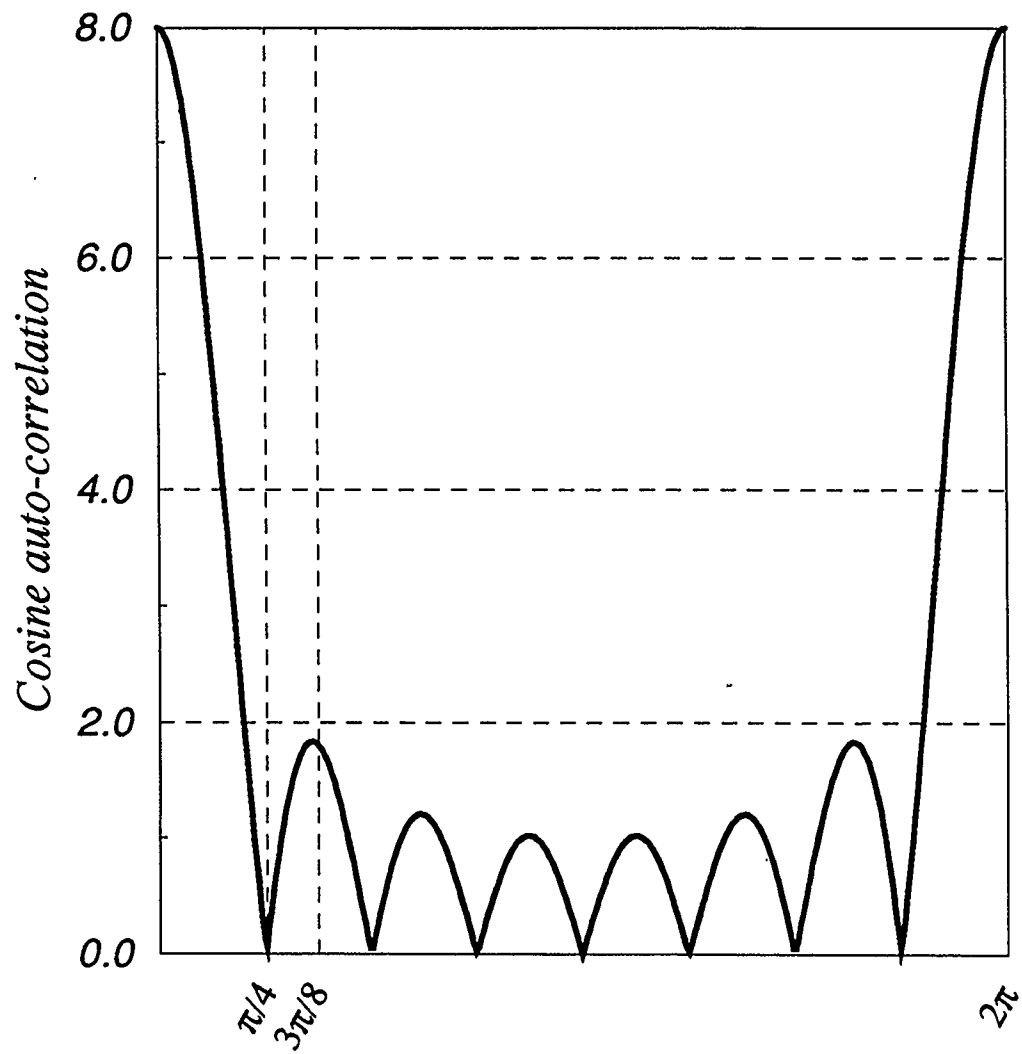


Figure A.2: Cosine auto-correlation function for $N = 8$.

Numerical results support the above results. For larger N , these results are more precise.

Appendix B

FS-SS

B.1 Effect of Incremental Patterns in Code Sequences on Cosine Cross-correlation Function

Let us rewrite the cosine cross-correlation function (equation (3.1)) here:

$$CR(\phi, \Theta) = \left| \sum_{i=0}^{N-1} \exp(i\phi + \theta_i) \right|$$

Now assume there is an incremental pattern in the phase sequence Θ , i.e.:

$$\theta_{N_1+i} = \theta_i + \psi \quad \text{for } i = 0, \dots, N_2$$

where $2N_1 < N_2 < N - N_1 - 1$. If $N_2 = nN_1 + N_3$, $CR(\phi, \Theta)$ can be arranged as:

$$\begin{aligned} CR(\phi, \Theta) &= \left| \sum_{i=0}^{N_1-1} \exp[j(i\phi + \theta_i)] + \sum_{i=N_1}^{2N_1-1} \exp[j(i\phi + \theta_i)] \right. \\ &\quad \left. + \dots + \sum_{i=nN_1}^{(n+1)N_1-1} \exp[j(i\phi + \theta_i)] + \sum_{i=(n+1)N_1}^{N-1} \exp[j(i\phi + \theta_i)] \right| \\ &= \left| \sum_{i=0}^{N_1-1} \exp[j(i\phi + \theta_i)] \right| \left| 1 + \exp[j(N_1\phi + \psi)] + \dots + \exp[jn(N_1\phi + \psi)] \right| \end{aligned} \tag{B.1}$$

the second factor in equation (B.1) will have a value of $n + 1$ when

$$N_1\phi + \psi = 2K\pi \longrightarrow \phi = \frac{2K\pi - \psi}{N_1}$$

where K is an integer. The variation rate of the first factor of B.1 is N_1 times smaller than that of the second factor, therefore quite likely, a maximum of the first factor may happen at the time the second factor is close to $n + 1$. Such a situation results in some large peaks in $CR(\phi, \Theta)$.

B.2 Proof of Lemma 3.1

$$\begin{aligned}
 R(\phi, -s) &= \left| \sum_{i=0}^{N-1} \exp[j(i\phi - (2\pi/L)s_i)] \right| \\
 &= \left| \sum_{i=0}^{N-1} \exp[j(-i\phi + (2\pi/L)s_i)] \right| \\
 &= R(-\phi, s)
 \end{aligned}$$

Note if $\max[R(\phi, -s)]$ happens at $\phi = \phi_{max}$, the same maximum occurs for $\max[R(\phi, s)]$ at $\phi = -\phi_{max}$. Therefore:

$$\max[R(\phi, -s)] = \max[R(\phi, s)]$$

Appendix C

Co-user Interference In FS-SS And OFS-SS Using Square Root Raised Cosine Signaling

To simplify calculation of co-user interferences in FS-SS, the following notes are helpful.

Random variables d_l, d_{l-n}, ϕ_{IF} and τ for any non-zero n are independent, and we have:

$$\overline{d_l} = 0, \quad \overline{d_l^2} = 1 \quad (\text{C.1})$$

and also:

$$\overline{d_l d_{l-n}} = 0, \quad n \neq 0 \quad (\text{C.2})$$

$$\overline{\exp[j(\phi_{IF} + \beta)]} = \int_0^{2\pi} \exp[j(K\phi_{IF} + \beta)] d(\phi_{IF}) = 0 \quad (\text{C.3})$$

where K is a non-zero integer and β is an arbitrary deterministic or random (independent of ϕ_{IF}) phase. These relations allow us, in averaging, to substitute with zero any components having a factor of d_l , or any sine or cosine having ϕ_{IF} in its argument, while averaging.

C.1 Co-user Interference in Non-Overlapping FS-SS

Using equation (2.15), one can write:

$$\begin{aligned}
I^2(0) = & \left[\sum_{n=-\infty}^{+\infty} d_n^2 g^2(nT - \tau_l) + \sum_{n_1=-\infty}^{+\infty} \sum_{\substack{n_2=-\infty \\ n_2 \neq n_1}}^{+\infty} d_{n_1} d_{n_2} g(n_1T - \tau_l) g(n_2T - \tau_l) \right] \\
& \left[\sum_{i=0}^{N-1} \cos^2(i\omega_d \tau_l + \phi_{IF} + \theta_i^{l0}) \right. \\
& \left. + 2 \sum_{i_1=0}^{N-2} \sum_{i_2=i_1+1}^{N-1} \cos(i_1\omega_d + \phi_{IF} + \theta_{i_1}^{l0}) \cos(i_2\omega_d + \phi_{IF} + \theta_{i_2}^{l0}) \right]
\end{aligned}$$

Now averaging $I_l^2(0)$ over ϕ_{IF} and d_n and using equations (C.2) and (C.3), causes a number of components to be zero, and the following equation results:

$$\overline{I_l^2(0)} = \lim_{T_u \rightarrow \infty} \frac{1}{T_u} \int_{-T_u/2}^{T_u/2} \left[\sum_{n=-\infty}^{+\infty} g^2(nT - \tau_l) \right] \left[\frac{N}{2} + \sum_{i_1=0}^{N-2} \sum_{i_2=i_1+1}^{N-1} \cos((i_1 - i_2)\omega_d \tau_l + \theta_{i_1}^{l0} - \theta_{i_2}^{l0}) \right] d\tau_l \quad (C.4)$$

To obtain an answer for above integral, the two integrals for I_g and I_w should be solved as follows.

$$I_g = \lim_{T_u \rightarrow \infty} \frac{1}{T_u} \int_{-T_u/2}^{T_u/2} \sum_{n=-\infty}^{\infty} g^2(nT - \tau_l) d\tau_l$$

$g(\tau_l)$ has the shape of raised cosine signal:

$$g(t) = \frac{\cos(\pi \frac{\alpha}{T} t)}{1 - (2\frac{\alpha}{T} t)^2} \left(\frac{\sin(\frac{\pi \alpha}{2T} t)}{\frac{\pi \alpha}{2T} t} \right)$$

and therefore it can easily be concluded that $g_s(\tau_l) = \sum_{n=-\infty}^{\infty} g^2(nT - \tau_l)$ is a periodic signal respect to τ_l with period T and therefore averaging over an infinite range will be the same as averaging on range $(0, T)$. Interchanging linear operations \int and \sum , and using superposition one can obtain:

$$\begin{aligned}
I_g &= \frac{1}{T} \int_{-T/2}^{T/2} \sum_{n=-\infty}^{\infty} g^2(nT - \tau_l) d\tau_l \\
&= \frac{1}{T} \sum_{n=-\infty}^{\infty} \int_{-T/2}^{T/2} g^2(nT - \tau_l) d\tau_l \\
&= \frac{1}{T} \int_{-\infty}^{\infty} g^2(\tau_l) d\tau_l
\end{aligned}$$

Using parseval's theorem, Ig is:

$$Ig = \frac{1}{T} \int_{f=-\infty}^{\infty} G^2(f) df \quad (\text{C.5})$$

where $G(f)$ is a raised cosine signal in frequency domain:

$$G(f) = \begin{cases} T & |f| < \frac{1-\alpha}{2T} \\ \frac{T}{2} \{1 - \sin[\pi \frac{T}{\alpha} (|f| - \frac{1}{2T})]\} & \frac{1-\alpha}{2T} < |f| < \frac{1+\alpha}{2T} \\ 0 & |f| > \frac{1+\alpha}{2T} \end{cases}$$

Substituting $G(f)$ in equation (C.5), Ig is obtained:

$$Ig = 1 - \frac{\alpha}{4} \quad (\text{C.6})$$

Iw is another integral which should be solved before obtaining the final answer for $\overline{I_i^2(0)}$:

$$Iw = \lim_{T_u \rightarrow \infty} \frac{1}{T_u} \int_{-T_u/2}^{T_u/2} g_s(\tau) \cos[i\omega_d \tau + \theta] d\tau$$

where i is a non-zero integer. The above integral is similar to the real part of Fourier transform of $g_s(t)$ at $\omega = \omega_d$. $g_s(\tau)$ can be written as:

$$g_s(\tau) = g^2(\tau) * \left[\sum_{n=-\infty}^{\infty} \delta(nT - \tau) \right]$$

which one may view as a result of filtering the signal $e(\tau) = [\sum_{n=-\infty}^{\infty} \delta(nT - \tau)]$ by filter with impulse response $g^2(\tau)$. Now the Fourier transform of $g_s(\tau)$ is:

$$G_s(f) = \mathcal{F}\{g^2(\tau)\} \left[\sum_{k=-\infty}^{\infty} \delta(\omega - \frac{k}{T}) \right]$$

where \mathcal{F} is the Fourier transform operator. Fourier transform maps multiplication operation onto convolution, therefore:

$$\mathcal{F}\{g^2(\tau)\} = G(f) * G(f)$$

Since the baseband bandwidth of $G(f)$ is $\frac{1+\alpha}{2T}$, the maximum bandwidth of $\mathcal{F}\{g^2(\tau)\}$ is $\frac{1+\alpha}{T}$. Therefore, since in non-overlapping FS-SS $f_d \geq \frac{1+\alpha}{T}$, the following result is obtained:

$$G_s(if_d) = 0$$

and subsequently :

$$Iw = 0. \quad (\text{C.7})$$

Note that $Iw = 0$ regardless of the choice of the pulse shape, and consequently, in non-overlapping FS-SS we have:

$$\overline{I_t^2(0)} = \frac{N}{2} Ig$$

and in the case of SRRC signaling:

$$\overline{I_t^2(0)} = \frac{N}{2} \left(1 - \frac{\alpha}{4}\right).$$

C.2 Co-user Interference in Overlapping FS-SS

Since SRRC filter is low pass, the co-user signal at the matched filter output ($J_l(t)$) is the same as $y_l(t)$ in equation (2.9). Using Euler's formula in equation (2.9), and noting that:

$$d_i(t - \tau_l) = \sum_{k=-\infty}^{\infty} d_k p(t - kT - \tau)$$

the following relation is obtained:

$$\begin{aligned} J_l(T_0) = & sp_0(T_0) [\sum_{i=0}^{N-1} \cos(\psi_i^0)] \\ & + sp_1(T_0) \{ \sum_{i=1}^{N-1} [\exp(j\psi_i^1) + \exp(j\psi_i^2)] \} \\ & + sp_2(T_0) \{ \sum_{i=1}^{N-1} [\exp(-j\psi_i^1) + \exp(-j\psi_i^2)] \} \end{aligned} \quad (\text{C.8})$$

where

$$\begin{aligned}
\psi_i^0 &= (\theta_i^0 - \theta_i^1) + \phi_{IF} + i\omega_d\tau \\
\psi_i^1 &= (\theta_i^0 - \theta_{i-1}^1) + \phi_{IF} + (i-1)\omega_d\tau \\
\psi_i^2 &= (\theta_i^1 - \theta_{i-1}^0) - \phi_{IF} - i\omega_d\tau
\end{aligned} \tag{C.9}$$

and

$$\begin{aligned}
sp_0(T_0) &= \sum_{k=-\infty}^{\infty} [d_k p(t - kT - \tau) * p(-t)]|_{t=T_0} \\
sp_1(T_0) &= \sum_{k=-\infty}^{\infty} d_k [p(t - kT - \tau) \exp(j2\pi f_d t)] * p(-t)|_{t=T_0} \\
sp_2(T_0) &= \sum_{k=-\infty}^{\infty} d_k [p(t - kT - \tau) \exp(-j2\pi f_d t)] * p(-t)|_{t=T_0}
\end{aligned} \tag{C.10}$$

It is easily seen that averaging $J_l(T_0)$ on d_k or ϕ_{IF} results in:

$$\overline{J_l} = 0$$

Since $g(t)$ is a real signal, we have:

$$sp_1(T_0) = sp_2^*(T_0) \tag{C.11}$$

where $*$, represents complex conjugate operation. From equations (C.8), (C.9), (C.10) and (C.11), the following relation is obtained for $J_l^2(T_0)$:

$$J_l^2(T_0) = J_{1l} + J_{2l} + J_{3l} + J_{4l} \tag{C.12}$$

where J_{1l}, J_{2l}, J_{3l} and J_{4l} are:

$$\begin{aligned}
J_{1l} &= [sp_0^2(T_0)] \left\{ \frac{1}{2} \sum_{i_1=0}^{N-1} \sum_{i_2=0}^{N-1} [\cos(\psi_{i_1}^0 - \psi_{i_2}^0) + \cos(\psi_{i_1}^0 + \psi_{i_2}^0)] \right\} \\
J_{2l} &= 2\text{Re} \left\{ \frac{1}{4} [sp_1^2(T_0)] \left\{ \sum_{i_1=1}^{N-1} \sum_{i_2=1}^{N-1} [\exp[j(\psi_{i_1}^1 + \psi_{i_2}^1)] + \exp[j(\psi_{i_1}^2 + \psi_{i_2}^2)]] \right. \right. \\
&\quad \left. \left. + 2 \sum_{i_1=1}^{N-1} \sum_{i_2=1}^{N-1} \exp[j(\psi_{i_1}^1 + \psi_{i_2}^2)] \right\} \right\}
\end{aligned}$$

$$\begin{aligned}
J_{3l} &= \frac{1}{2} |sp_1(T_0)|^2 \left\{ \sum_{i_1=1}^{N-1} \sum_{i_2=1}^{N-1} [\exp[j(\psi_{i_1}^1 - \psi_{i_2}^1)] + \exp[j(\psi_{i_1}^2 - \psi_{i_2}^2)]] \right. \\
&\quad \left. + \sum_{i_1=1}^{N-1} \sum_{i_2=1}^{N-1} [\exp[j(\psi_{i_1}^1 - \psi_{i_2}^2)] + \exp[-j(\psi_{i_1}^1 - \psi_{i_2}^2)]] \right\} \\
J_{4l} &= 2Re\left\{ \frac{1}{2} [sp_0(T_0)sp_1(T_0)] \left\{ \sum_{i_1=0}^{N-1} \sum_{i_2=1}^{N-1} [\exp[j(\psi_{i_1}^0 + \psi_{i_2}^1)] + \exp[j(\psi_{i_1}^0 + \psi_{i_2}^2)]] \right. \right. \\
&\quad \left. \left. + \sum_{i_1=0}^{N-1} \sum_{i_2=1}^{N-1} [\exp[j(-\psi_{i_1}^0 + \psi_{i_2}^1)] + \exp[j(-\psi_{i_1}^0 + \psi_{i_2}^2)]] \right\} \right\}
\end{aligned}$$

Averaging on d_k and ϕ_{IF} , forces a number of elements in J_{1l}, J_{2l}, J_{3l} and J_{4l} to be zero. Consequently, $\overline{J_l^2(T_0)}$ reduces to:

$$\overline{J_l^2(T_0)} = \overline{J_{1l}(T_0)} + \overline{J_{2l}(T_0)} + \overline{J_{3l}(T_0)} + \overline{J_{4l}(T_0)} \quad (C.13)$$

where

$$\begin{aligned}
J_{1l}(T_0) &= [sg_1] \frac{1}{4} \left\{ \sum_{i_1=0}^{N-1} \sum_{i_2=0}^{N-1} [\exp[j(\psi_{i_1}^0 - \psi_{i_2}^0)] + \exp[-j(\psi_{i_1}^0 - \psi_{i_2}^0)]] \right\} \\
J_{2l}(T_0) &= Re\{[sg_2] \left[\sum_{i_1=1}^{N-1} \sum_{i_2=1}^{N-1} \exp[j(\psi_{i_1}^1 + \psi_{i_2}^2)] \right]\} \\
J_{3l}(T_0) &= \frac{1}{2} [sg_3] \left\{ \sum_{i_1=1}^{N-1} \sum_{i_2=1}^{N-1} [\exp[j(\psi_{i_1}^1 - \psi_{i_2}^2)] + \exp[-j(\psi_{i_1}^1 - \psi_{i_2}^2)]] \right\} \\
J_{4l}(T_0) &= Re\{[sg_4] \left\{ \sum_{i_1=0}^{N-1} \sum_{i_2=1}^{N-1} [\exp[j(\psi_{i_1}^0 + \psi_{i_2}^2)] + \exp[j(-\psi_{i_1}^0 + \psi_{i_2}^1)]] \right\}\}
\end{aligned}$$

in which sg_1, sg_2, sg_3 and sg_4 are:

$$\begin{aligned}
sg_1 &= \sum_{-\infty}^{\infty} [p(t - kT - \tau) * p(-t)]^2 |_{t=T_0} \\
sg_2 &= \sum_{-\infty}^{\infty} \{ [p(t - kT - \tau) \exp(j2\pi f_d t)] * p(-t) \}^2 |_{t=T_0} \\
sg_3 &= \sum_{-\infty}^{\infty} | [p(t - kT - \tau) \exp(j2\pi f_d t)] * p(-t) |^2 |_{t=T_0} \\
sg_4 &= \sum_{-\infty}^{\infty} \{ [p(t - kT - \tau) * p(-t)] \\
&\quad [[p(t - kT - \tau) \exp(j2\pi f_d t)] * p(-t)] \} |_{t=T_0}
\end{aligned}$$

Using the inverse Fourier transform relation ($x(t) = \int_{-\infty}^{\infty} X(f) \exp(j2\pi ft)df$), they can be rewritten as:

$$\begin{aligned}
sg_1 &= \sum_{k=-\infty}^{\infty} \left[\int_{f=-\infty}^{\infty} \exp[-j2\pi f(kT + \tau)] P(f) P^*(f) \exp(j2\pi fT_0) df \right]^2 \\
sg_2 &= \sum_{k=-\infty}^{\infty} \left[\int_{f=-\infty}^{\infty} \exp[-j2\pi(f - f_d)(kT + \tau)] P(f - f_d) P^*(f) \exp(j2\pi fT_0) df \right]^2 \\
sg_3 &= \sum_{k=-\infty}^{\infty} \left| \int_{f=-\infty}^{\infty} \exp[-j2\pi(f - f_d)(kT + \tau)] P(f - f_d) P^*(f) \exp(j2\pi fT_0) df \right|^2 \\
sg_4 &= \sum_{k=-\infty}^{\infty} \left\{ \left[\int_{f=-\infty}^{\infty} \exp[-j2\pi f(kT + \tau)] P(f) P^*(f) df \right] \right. \\
&\quad \left. \left[\int_{f=-\infty}^{\infty} \exp[-j2\pi(f - f_d)(kT + \tau)] P(f - f_d) P^*(f) \exp(j2\pi fT_0) df \right] \right\}
\end{aligned}$$

Comparing equations (2.19) and (C.13), the three different components of equation (2.19) are found to be:

$$\begin{aligned}
\overline{M_i^2(T_0)} &= \overline{J_{11}(T_0)} \\
\overline{O_i^2(T_0)} &= \overline{J_{21}(T_0)} + \overline{J_{31}(T_0)} \\
\overline{2M_i^2(T_0)O_i^2(T_0)} &= \overline{J_{41}(T_0)}
\end{aligned}$$

To obtain $\overline{J_{11}(T_0)}$, $\overline{J_{21}(T_0)}$, $\overline{J_{31}(T_0)}$ and $\overline{J_{41}(T_0)}$, the following four integrals should be solved.

$$z_m(n) = \lim_{T_u \rightarrow \infty} \frac{1}{T_u} \int_{-T_u/2}^{T_u/2} sg_m \exp(j2\pi n f_d \tau) d\tau \quad \text{for } m = 1, 2, 3, 4 \quad (\text{C.14})$$

The following two relations (equations (C.15) and (C.16)) help us to simplify $z_m(n)$ for numerical solution.

$$\left[\int_{f=f_a}^{f_A} A(f) df \right] \left[\int_{f=f_b}^{f_B} B(f) df \right] = \left[\int_{f_1=f_a}^{f_A} \int_{f_2=f_b}^{f_B} A(f_1) B(f_2) df_1 df_2 \right] \quad (\text{C.15})$$

$$\frac{1}{T_u} \int_{\tau=-T_u/2}^{T_u/2} \exp(ja\tau) d\tau = \frac{\sin(aT_u/2)}{aT_u/2} = \text{sinc}(aT_u/2) \quad (\text{C.16})$$

Substituting sg_m in equation (C.14), and using last two relations, one can arrive at the following equations for $z_m(n)$, $m = 1, 2, 3, 4$:

$$z_1(n) = \sum_{k=-\infty}^{\infty} \lim_{T_u \rightarrow \infty} \int_{f_1=-f_w}^{f_w} \int_{f_2=-f_w}^{f_w} |P(f_1)|^2 |P(f_2)|^2 \text{sinc}[\pi(f_1 + f_2 - n f_d) T_u] \exp[-j2\pi(f_1 + f_2)(kT - T_0)] df_1 df_2 \quad (\text{C.17})$$

$$z_2(n) = \sum_{k=-\infty}^{\infty} \lim_{T_u \rightarrow \infty} \int_{f_1=f_d-f_w}^{f_w} \int_{f_2=f_d-f_w}^{f_w} P(f_1 - f_d) P^*(f_1) P(f_2 - f_d) P^*(f_2) \text{sinc}[\pi(f_1 + f_2 - (2 + n) f_d) T_u] \exp[-j2\pi(f_1 + f_2 - 2f_d) kT] \exp[j2\pi(f_1 + f_2) T_0] df_1 df_2 \quad (\text{C.18})$$

$$z_3(n) = \sum_{k=-\infty}^{\infty} \lim_{T_u \rightarrow \infty} \int_{f_1=f_d-f_w}^{f_w} \int_{f_2=f_d-f_w}^{f_w} P(f_1 - f_d) P^*(f_1) P^*(f_2 - f_d) P(f_2) \text{sinc}[\pi(f_1 - f_2 - n f_d) T_u] \exp[-j2\pi(f_1 - f_2)(kT - T_0)] df_1 df_2 \quad (\text{C.19})$$

$$z_4(n) = \sum_{k=-\infty}^{\infty} \lim_{T_u \rightarrow \infty} \int_{f_1=-f_w}^{f_w} \int_{f_2=f_d-f_w}^{f_w} P(f_1) P^*(f_1) P(f_2 - f_d) P^*(f_2) \text{sinc}[\pi(f_1 + f_2 - (1 + n) f_d) T_u] \exp[-j2\pi(f_1 + f_2 - f_d) kT] \exp[j2\pi(f_1 + f_2) T_0] df_1 df_2 \quad (\text{C.20})$$

where $f_w = W/2\pi$ is the baseband bandwidth of the signal $P(f)$. Equations (C.17), (C.18), (C.19), and (C.20) are general in the sense that $P(f)$ can be any bandlimited spectrum with bandwidth $f_w < f_d$, and also they can be easily solved numerically. In numerical analysis of each $z_m(n)$, depending on pulse shape $p(t)$, sufficiently large value of T_u should be chosen; also since for most pulse shapes $p(t) = 0$ for $t > t_{max}$, summation needs to be done for a few values of k only.

For SRRC signaling, without loss of generality $P(f)$ can be assumed real because any non-zero phase for $P(f)$ is a result of delay, which can be absorbed in other

exponentials in $z_m(n)$. Numerical evaluation of $z_m(n)$ s reveals the following results.

$z_1(n)$:

$z_1(n) = 0$ for any non-zero n , except for the case when $f_d = 1/T$. Also $z_1(0)$ and $z_1(1)$ do not depend on T_0 . From these observations one can obtain the following result for $\overline{J_{1l}}$:

$$\overline{J_{1l}} = \frac{N}{2}z_1(0) + \frac{1}{2}z_1(1) \sum_{i=1}^{N-1} \exp[j(\theta_i^{0l} - \theta_{i-1}^{0l})]$$

If the phase sequences are chosen properly, the summation is small and the second term can be ignored. One may notice that $\overline{J_{1l}}$ is the interference caused by the main lobe of the co-user signal, therefore, as it is expected, the results match the co-user interferences in non-overlapping FS-SS.

$z_2(n)$:

$z_2(n) = 0$ for any value of n , and it does not depend on T_0 , therefore:

$$\overline{J_{2l}} = 0$$

$z_3(n)$:

$z_3(n) = 0$ for $n \neq 0$, and it is independent of T_0 , then:

$$\overline{J_{3l}} = (N - 1)z_3(0)$$

$z_4(n)$:

If $f_d \neq 1/T$, then $z_4(n) = 0$ for any non-zero n , and for $f_d = 1/T$, $z_4(-1) \neq 0$.

Although $z_4(0)$ and $z_4(-1)$ change with T_0 , their amplitude is independent of it.

Therefore:

$$\begin{aligned} \overline{J_{4l}} = & 2Re\{z_4(0) \sum_{i=1}^{N-1} \exp[j(\theta_i^0 - \theta_{i-1}^0)] \\ & + z_4(-1) \sum_{i=1}^{N-1} \exp[j(\theta_i^l - \theta_{i-1}^l)]\} \end{aligned}$$